



Article scientifique

Article

2020

Published version

Open Access

This is the published version of the publication, made available in accordance with the publisher's policy.

Lymphatic endothelial cells prime naïve CD8+ T cells into memory cells under steady-state conditions

Vokali, Efthymia; Yu, Shann S; Hirose, Sachiko; Rinçon-Restrepo, Marcela; Do Valle Duraes, Fernanda; Scherer, Stefanie; Corthésy-Henrioud, Patricia; Kilarski, Witold W; Mondino, Anna; Zehn, Dietmar; Hugues, Stéphanie; Swartz, Melody A

How to cite

VOKALI, Efthymia et al. Lymphatic endothelial cells prime naïve CD8+ T cells into memory cells under steady-state conditions. In: Nature Communications, 2020, vol. 11, n° 1, p. 538. doi: 10.1038/s41467-019-14127-9

This publication URL: <https://archive-ouverte.unige.ch/unige:144199>

Publication DOI: [10.1038/s41467-019-14127-9](https://doi.org/10.1038/s41467-019-14127-9)

ARTICLE

<https://doi.org/10.1038/s41467-019-14127-9>

OPEN

Lymphatic endothelial cells prime naïve CD8⁺ T cells into memory cells under steady-state conditions

Efthymia Vokali^{1,7}, Shann S. Yu^{1,2,7}, Sachiko Hirose¹, Marcela Rinçon-Restrepo¹, Fernanda V. Duraes³, Stefanie Scherer⁴, Patricia Corthésy-Henrioud¹, Witold W. Kilarski^{1,2}, Anna Mondino⁵, Dietmar Zehn⁴, Stéphanie Hugues³ & Melody A. Swartz^{1,2,6*}

Lymphatic endothelial cells (LECs) chemoattract naïve T cells and promote their survival in the lymph nodes, and can cross-present antigens to naïve CD8⁺ T cells to drive their proliferation despite lacking key costimulatory molecules. However, the functional consequence of LEC priming of CD8⁺ T cells is unknown. Here, we show that while many proliferating LEC-educated T cells enter early apoptosis, the remainders comprise a long-lived memory subset, with transcriptional, metabolic, and phenotypic features of central memory and stem cell-like memory T cells. In vivo, these memory cells preferentially home to lymph nodes and display rapid proliferation and effector differentiation following memory recall, and can protect mice against a subsequent bacterial infection. These findings introduce a new immunomodulatory role for LECs in directly generating a memory-like subset of quiescent yet antigen-experienced CD8⁺ T cells that are long-lived and can rapidly differentiate into effector cells upon inflammatory antigenic challenge.

¹Institute of Bioengineering, École Polytechnique Fédérale de Lausanne (EPFL), Lausanne, Switzerland. ²Pritzker School of Molecular Engineering, University of Chicago, Chicago, IL, USA. ³Department of Pathology and Immunology, Faculty of Medicine, University of Geneva, Geneva, Switzerland. ⁴Swiss Vaccine Research Institute, Epalinges, Switzerland. ⁵Division of Immunology, Transplantation and Infectious Diseases, San Raffaele Scientific Institute, Milan, Italy. ⁶Ben May Department of Cancer Research, University of Chicago, Chicago, IL, USA. ⁷These authors contributed equally: Efthymia Vokali, Shann S. Yu.
*email: melodyswartz@uchicago.edu

The lymphatic endothelium is actively involved in shaping T cell responses, both directly and indirectly^{1–6}. In the lymph nodes (LNs), lymphatic endothelial cells (LECs) have been shown to present peripheral tissue-restricted antigens on MHC class I molecules (MHCI) to induce tolerance in autoreactive CD8⁺ T cells^{7,8}. In addition to endogenous antigen presentation, we and others have demonstrated that LECs abundantly scavenge and can cross-present exogenous antigens to naïve CD8⁺ T cells and drive proliferation, both in the context of a tumor⁹ as well as under homeostatic conditions¹⁰. These LEC-activated T cells lack effector cytokine secretion and some undergo early-generation apoptosis, suggesting a dysfunctional or anergic phenotype. LECs have therefore been established as antigen-presenting cells (APCs) that can sample the peripheral exogenous antigen repertoire and contribute to CD8⁺ T cell regulation and tolerance.

The induction of peripheral tolerance has been primarily assigned to professional APCs¹¹. Under homeostatic conditions, LN-resident immature dendritic cells (DCs) acquire self-antigens from peripheral tissues and cross-present them without co-stimulation, inducing T cell anergy or deletion¹². In this case, peripherally tolerized CD8⁺ T cells remain functionally impaired, even in response to pathogenic challenge¹³. In contrast, apparently tolerized CD8⁺ T cells that were primed by non-hematopoietic cells—such as intestinal epithelial cells and liver sinusoidal endothelial cells (LSECs)—can exit the non-responsive state and be functionally reactivated under pro-inflammatory conditions^{14,15}. We therefore asked whether quiescent LEC-educated CD8⁺ T cells can be functionally activated upon inflammatory challenge, thereby representing a memory-like state rather than an irreversibly anergic or tolerized state.

Canonically, memory T cells are considered to arise during the contraction phase of an immune response (e.g., after primary infection or vaccination), differentiated from a subset of effector T cells. However, other models propose that memory T cells can arise directly from naïve cells, either as precursors to effector memory and effector T cells (i.e., the loss of memory correlates with terminal differentiation), or as asymmetric divisions reminiscent of stem cell behavior^{16,17}. The memory T cell pool is also highly heterogeneous, as their phenotypic state is tightly governed by the integration of numerous signals including antigen load and persistence, TCR affinity, co-stimulation, cytokine environment, and CD4⁺ T cell help^{16–18}. An emerging consensus suggests that higher levels of TCR–pMHC affinity, antigen load, co-stimulation, and pro-inflammatory cytokines promote differentiation into terminal effectors, while weaker activation signals promote a shift towards memory T cells¹⁹. This new understanding raises important considerations with regard to CD8⁺ T cell priming by LECs and other non-hematopoietic cells, which occurs in the context of lower levels of co-stimulation and pro-inflammatory cytokines and higher levels of co-inhibitory signals relative to priming by activated DCs¹⁰.

Here, we describe a new role for LECs in directly cross-priming naïve CD8⁺ T cells into long-lived memory T cells capable of potent effector differentiation following inflammatory challenges. This has implications for understanding T cell memory and also helps to reconcile the seemingly contradictory roles of lymphangiogenesis in tumors versus in chronic inflammatory diseases or transplantation. We suggest that LEC-educated T cells may function as a reserve of antigen-experienced T cells in a memory-like state, enhancing immune responses upon immunogenic challenge or promoting tolerance upon challenge under immunosuppressive conditions, as in the tumor microenvironment.

Results

Priming by stromal cells promotes CD8⁺ T cell memory. First, we sought to determine the relevance of antigen uptake and

cross-presentation by LECs on CD8⁺ T cell responses in vivo. Creating mice in which MHCI presentation is restricted to LECs was not feasible, since there is no known truly lymphatic-specific gene (e.g., *Lyve1* is expressed by macrophage subsets, *Prox1* by hepatocytes, and podoplanin (*Pdpn*) by fibroblast subsets). Instead, we generated bone marrow chimeric mice in which donor CD45⁺ cells lacked MHCI ($\beta_2m^{-/-}$:WT, denoting the status of the hematopoietic population:non-hematopoietic remainder of the host), and therefore presentation of the H-2K^b-restricted SIINFEKL epitope after intradermal (i.d.) injection of OVA would be restricted to radioresistant lymph node stromal cells (LNSCs). LNSCs include fibroblastic reticular cells (FRCs), follicular DCs, and blood endothelial cells (BECs) as well as LECs. However, among these LNSC subtypes, LECs take up the majority of antigen in the draining LNs (dLNs) following i.d. administration under steady-state conditions¹⁰. Furthermore, when loaded with antigen ex vivo, FRCs induced negligible T cell proliferation in vitro compared to LECs (Supplementary Fig. 1). We therefore reasoned that LECs would be the primary Ag-presenting cells for OVA following i.d. administration in $\beta_2m^{-/-}$:WT chimeric mice, with little contribution from FRCs^{9,20}. As controls, we also generated inverse chimeras (WT: $\beta_2m^{-/-}$) as well as positive (WT:WT) and negative ($\beta_2m^{-/-}$: $\beta_2m^{-/-}$) controls.

We transferred naïve CFSE-labeled OT-I CD8⁺ T cells (CD45.1/2⁺) intravenously (i.v.) into the mice and the following day administered i.d. OVA (50 μ g) or PBS (Fig. 1a). Five days later, we analyzed the OT-I cells in skin-dLNs and observed substantial levels of antigen-specific proliferation in $\beta_2m^{-/-}$:WT mice compared to those injected with PBS, suggesting that indeed, MHCI-antigen presentation by LNSCs can induce T cell proliferation in vivo (Fig. 1b). As expected, transferred OT-I cells proliferated the most in WT:WT mice and the least in $\beta_2m^{-/-}$: $\beta_2m^{-/-}$ mice, while interestingly, proliferation was comparable in WT: $\beta_2m^{-/-}$ and $\beta_2m^{-/-}$:WT mice (both ~70% of levels in WT:WT mice), indicating that LNSC participation in T cell priming under steady-state conditions is important and physiologically relevant compared to that induced by DCs and other hematopoietic cells.

Next, we evaluated the phenotype of the LNSC-educated OT-I cells. In all mice except $\beta_2m^{-/-}$: $\beta_2m^{-/-}$ chimeras, the majority of transferred cells expressed CD44⁺ with both central memory (T_{CM} , CD44⁺CD62L⁺) and effector/effector memory ($T_{eff/EM}$, CD44⁺CD62L⁻) subsets in all groups (Fig. 1c). Interestingly, the T_{CM} fraction was highest in the $\beta_2m^{-/-}$:WT mice (Fig. 1d), where the ratio of T_{CM} to $T_{eff/EM}$ was close to unity (Fig. 1e), while in mice lacking MHCI on LNSC (WT: $\beta_2m^{-/-}$), ~30% of total OT-I cells were T_{CM} . Upon ex vivo SIINFEKL re-stimulation, the OT-I cell fractions that were IFN γ ⁺ or IL-2⁺ were similar among the groups (Fig. 1f, g), but the fraction of double-positive cells was lowest in WT: $\beta_2m^{-/-}$ mice (Fig. 1h) and the fraction of IFN γ ⁺ cells expressing IL-2 was highest in $\beta_2m^{-/-}$:WT mice (Fig. 1i). These results established that (i) LNSCs are capable of antigen presentation under non-inflammatory conditions to induce the proliferation and activation of CD8⁺ T cells, and (ii) T cell education by LNSCs promotes a memory phenotype.

LECs uniquely generate CD8⁺ memory. Although LECs represented the dominant LNSC subset that both take up i.d.-delivered antigen¹⁰ and can cross-present antigen to naïve CD8⁺ T cells (Supplementary Fig. 1), we could not rule out the unlikely possibility that migratory DCs such as Langerhans cells, which are less radiation-sensitive than circulating DCs²¹, could contribute to the memory skewing that we saw (although previous in vitro studies using co-cultures of such cells with CD8⁺ T cells did not recapitulate the phenotype we observed^{21–23}). To address this, we first exposed LN-resident cells to antigen in vivo and then tested

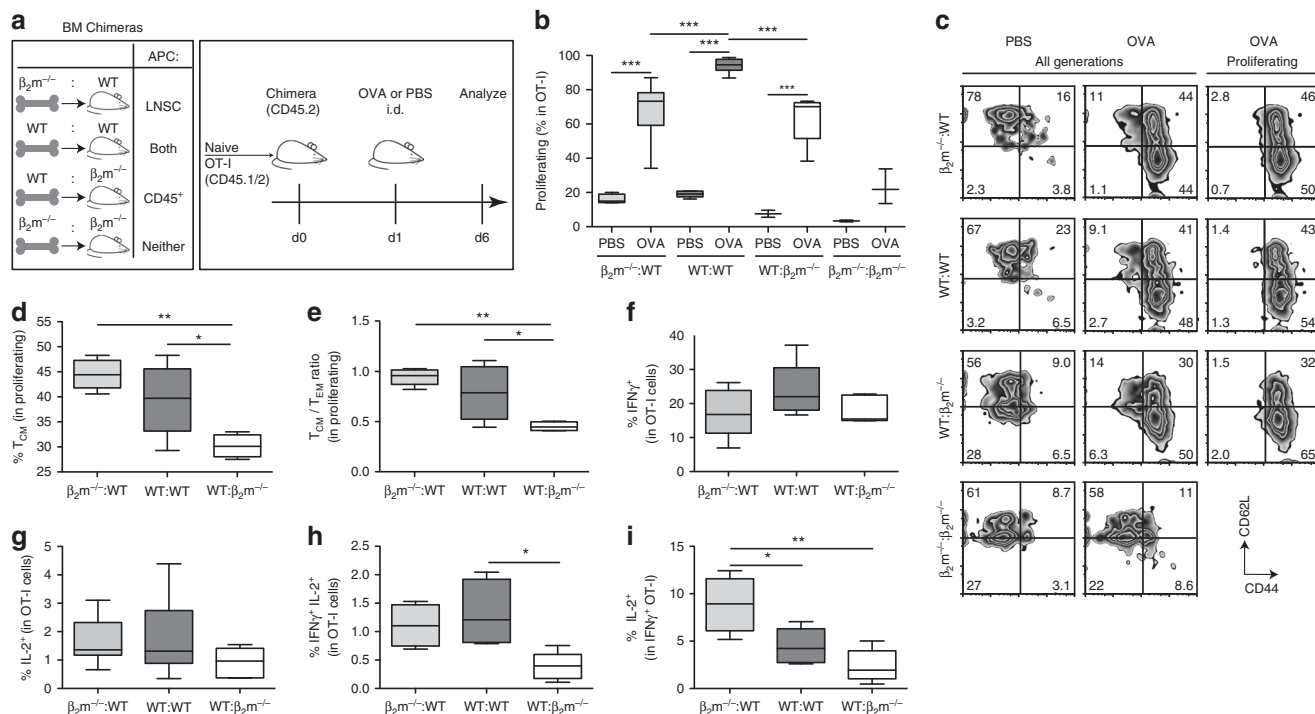


Fig. 1 CD8⁺ T cells educated by lymph node stromal cells display memory-like characteristics. **a** Experimental schematic, highlighting nomenclature for BM chimeras according to MHC1-competent cell types (left), and timeline (right) for transfer of CFSE-labeled OT-I cells (i.v.), OVA challenge (50 μ g; i.d.), and sacrifice. Skin-draining LNs were analyzed by flow cytometry. **b** Quantification of cell proliferation via CFSE dilution on transferred OT-I cells. **c** Representative contour plots of CD44 and CD62L expression gated on all transferred cells (left, center) or on proliferating transferred cells (right). **d, e** Phenotype of proliferating, transferred cells quantified according to **d** frequency of T_{CM} (CD44⁺CD62L⁺) and **e** the ratio of T_{CM} (CD44⁺CD62L⁺) to T_{eff/EM} (CD44⁺CD62L⁻). **f** Frequency of intracellular IFN γ^+ , **g** IL-2⁺, and **h** bifunctional IFN γ^+ IL-2⁺ cells among all transferred cells after 5 h ex vivo re-stimulation with SIINFEKL followed by intracellular staining. **i** Frequency of IL-2⁺ cells within IFN γ^+ OT-I cells. Representative data pooled from two independent experiments ($n = 3-5$ each). Whiskers: Min to Max, median. **c, e, f**; * $p \leq 0.05$, ** $p \leq 0.01$, *** $p \leq 0.001$ by one-way ANOVA followed by Bonferroni post-test.

their ability to activate cognate T cells ex vivo. Specifically, we injected WT mice i.d. with OVA or PBS, and after 2 h, isolated the dLNs and sorted for four subsets: DCs (CD45⁺ CD11c⁺), macrophages (M ϕ ; CD45⁺ F4/80⁺), LECs (CD45⁻ gp38⁺ CD31⁺), and FRCs (CD45⁻ gp38⁺ CD31⁻). These subsets (or antigen-pulsed, LPS-activated bone marrow-derived DCs (BMDCs) as a positive control) were immediately placed into culture with naïve OT-I CD8⁺ T cells for 3 days (Fig. 2a).

We reasoned that after 2 h, injected antigens would have already drained to and perfused the sinuses of the dLNs, whereas migratory DCs that picked up antigen from the skin would not yet have arrived²⁴⁻²⁶. Consistent with this, 71 \pm 4% of LECs were positive for antigen at this time, versus 14 \pm 4% of LN-resident DCs (Fig. 2b, c). Nevertheless, the antigen-positive DCs had taken up more antigen per cell than the antigen-positive LECs, showcasing their propensity to sample and internalize antigen (Fig. 2d).

Without antigen, overall OT-I cell survival was highest when co-cultured with LECs and lowest with FRCs, consistent with previous reports that LECs are the major source of the pro-survival cytokine IL-7 in the LN^{27,28}. With antigen, LECs were the only subset that increased T cell numbers (Fig. 2e) and activated T cells (Fig. 2f) relative to PBS. There was no appreciable increase in T cell numbers when cultured with DCs, presumably due to inefficient in vivo targeting of DCs compared to LECs after 2 h (Fig. 2c). As expected, the overall differences seen in OVA-treated vs. PBS-treated mice for all groups were small compared to when antigen pulsing is done

in vitro, where all of the cells would be exposed to antigen (Supplementary Fig. 1).

In addition, antigen education by LECs increased intracellular IFN γ^+ in OT-I CD8⁺ T cells (Fig. 2g). Interestingly, this was not reflected in the levels of IFN γ in the supernatant, which were low in all cultures compared to BMDC-educated T cells (Fig. 2h). On the other hand, IL-2 levels were significantly elevated in LEC and DC co-cultures from OVA-treated vs. PBS-treated mice. These results suggest that LEC education activates the CD8⁺ T cells to a state where they are poised to generate IFN γ without secreting it, while increasing secretion of IL-2 to support homeostatic proliferation and survival¹⁸.

We next explored the phenotype of these activated OT-I cells. Interestingly, the IFN γ^+ cells activated by LECs isolated from OVA-treated vs. PBS-treated mice occurred mainly in CD62L⁺ cells (Fig. 2i); indeed, the T_{CM} compartment accounted for ~55% of IFN γ^+ T cells (Fig. 2j). These IFN γ^+ OT-I cells also stained positively for other markers of memory cells, including the receptors to IL-2, IL-7, and IL-2/15 (CD25, CD127, and CD122, respectively) as well as the co-stimulatory receptor CD27 (Fig. 2k, l). Collectively, these data suggest that in the absence of inflammatory signals, antigen cross-presentation by LECs under steady-state conditions may directly promote CD8⁺ T cell memory.

To further test whether LECs can indeed promote the acquisition of a memory phenotype by CD8⁺ T cells in vivo, we designed a method to introduce β_2m -competent LECs into $\beta_2m^{-/-}$ mice, such that the transplanted LECs would be the sole

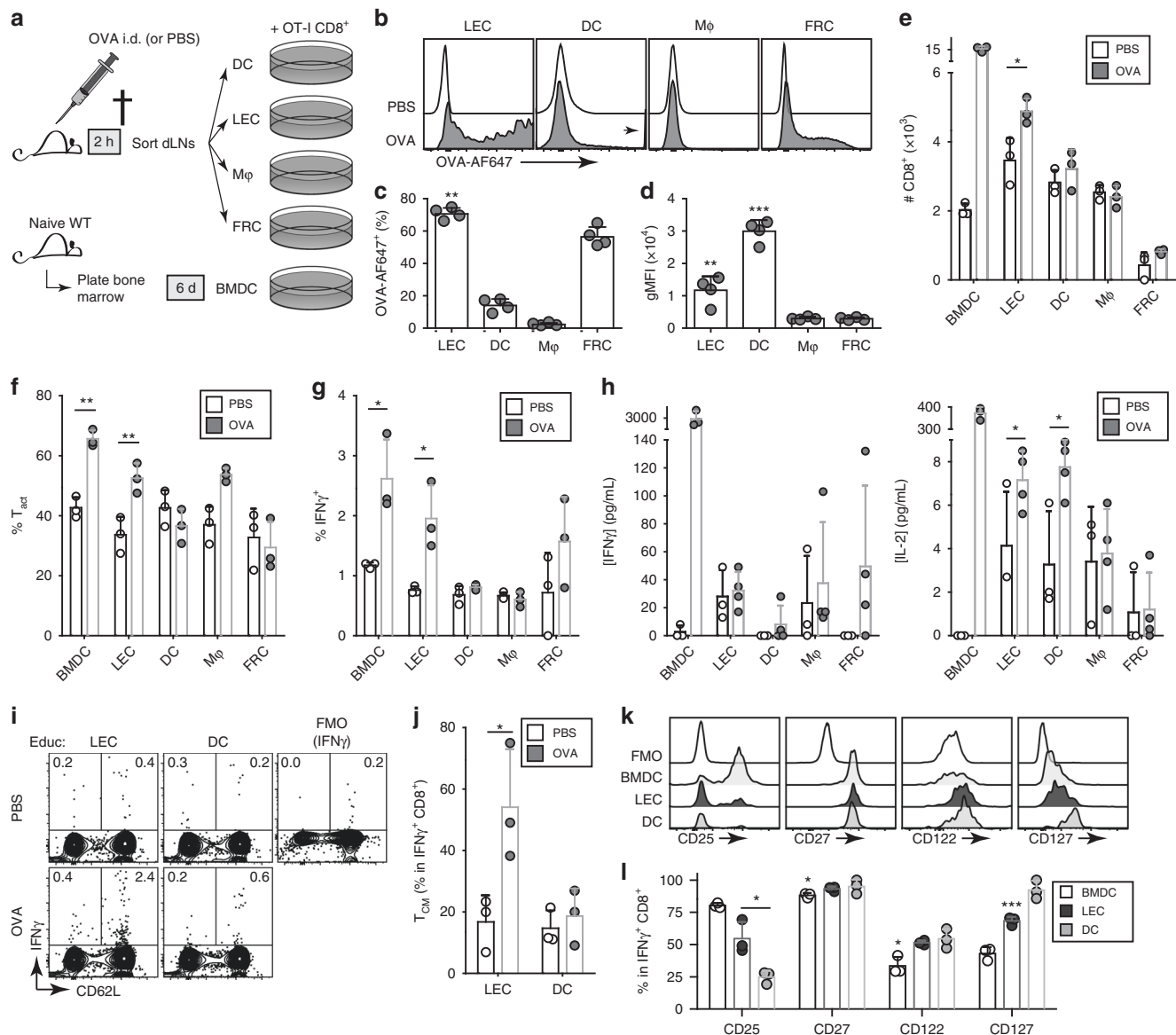


Fig. 2 LECs that had taken up antigen in vivo can activate T cells ex vivo. **a** Skin-draining LNs from OVA-challenged or control (PBS) mice were sorted for DCs (CD45⁺CD11c⁺), macrophages (Mφ; CD45⁺F4/80⁺), LECs (CD45⁺gp38⁺CD31⁺), and FRCs (CD45⁺gp38⁺CD31⁻), which were subsequently co-cultured with naïve OT-I CD8⁺ T cells for 3 days. As an assay positive control, OT-I cells were co-cultured with OVA/CpG-pulsed BMDCs and analyzed in parallel. **b–d** Cellular distribution of AF647-labeled OVA (OVA-AF647) at time of sacrifice. **b** Representative histograms, **c** quantification of frequency of OVA-AF647⁺ cells within indicated populations, and **d** OVA-AF647 MFI gated on OVA-AF647⁺ cells. **e** Absolute recovery of live OT-I cells and **f, g** frequency among all live OT-I cells of **f** activated phenotype (defined as being positive for CD25, CD44, or CD69) and **g** intracellular IFNγ⁺ expression. **h** Endpoint concentrations of IFNγ and IL-2 in the co-culture supernatants. **i** Representative contour plots depicting IFNγ versus CD62L expression of all live OT-I cells (inset numbers indicate percentage of cells within the gate), with **j** quantification of percentage of IFNγ⁺ OT-I cells that exhibit central memory-like (CD44⁺CD62L⁺; T_{CM}) phenotype. **k, l** Gating on IFNγ⁺ OT-I cells, the phenotype of activated, cytokine-producing cells was analyzed for a panel of memory cell-associated markers. **k** Representative histograms of expression of CD25 (IL-2Rα), CD27, CD122 (IL-2/15Rβ), and CD127 (IL-7Rα), quantified in **l** as a percentage of marker-positive cells among IFNγ⁺ OT-I cells. **p* < 0.05, ***p* < 0.01, ****p* < 0.001 via Student's *t*-test. Columns and error bars indicate mean ± SD for *n* = 3–4 from one of two independent experiments.

source of peptide-MHCI systemically. For such a system, we used LECs isolated from *Actb-mOVA* mice, where expression of membrane-bound OVA is driven by the β-actin promoter in all cells. We confirmed that in vitro, these LECs could stimulate the acquisition of CD44⁺CD62L⁺ phenotype by co-cultured naïve OT-I cells (Fig. 3a; 28 ± 13%, relative to 7.6 ± 0.4% with wild-type, unpulsed LECs), albeit to a lesser degree than OT-I cells co-cultured with OVA-pulsed control LECs (84 ± 2%).

In our hands, injections (i.d., intraperitoneal, intravascular) of LEC cell suspensions produced poor survival and recovery even

within 1 day post-administration, so we opted to produce 3D spheroid cultures for implantation, based on the observation that many endothelial cells maintain better structure and function in the presence of self-derived extracellular matrix proteins. Spheroids (18 ± 3 μm diameters) were implanted into i.d. pockets formed between the ear cartilage and the ventral skin (Fig. 3b), where they survived more than 8 days in fully immunocompetent mice (Fig. 3c). β₂m^{-/-} mice implanted with WT or OVA-expressing LEC spheroids later received a co-transfer of OT-I and bystander CD8⁺ T cells at a 1:5 ratio (Fig. 3d). While there were

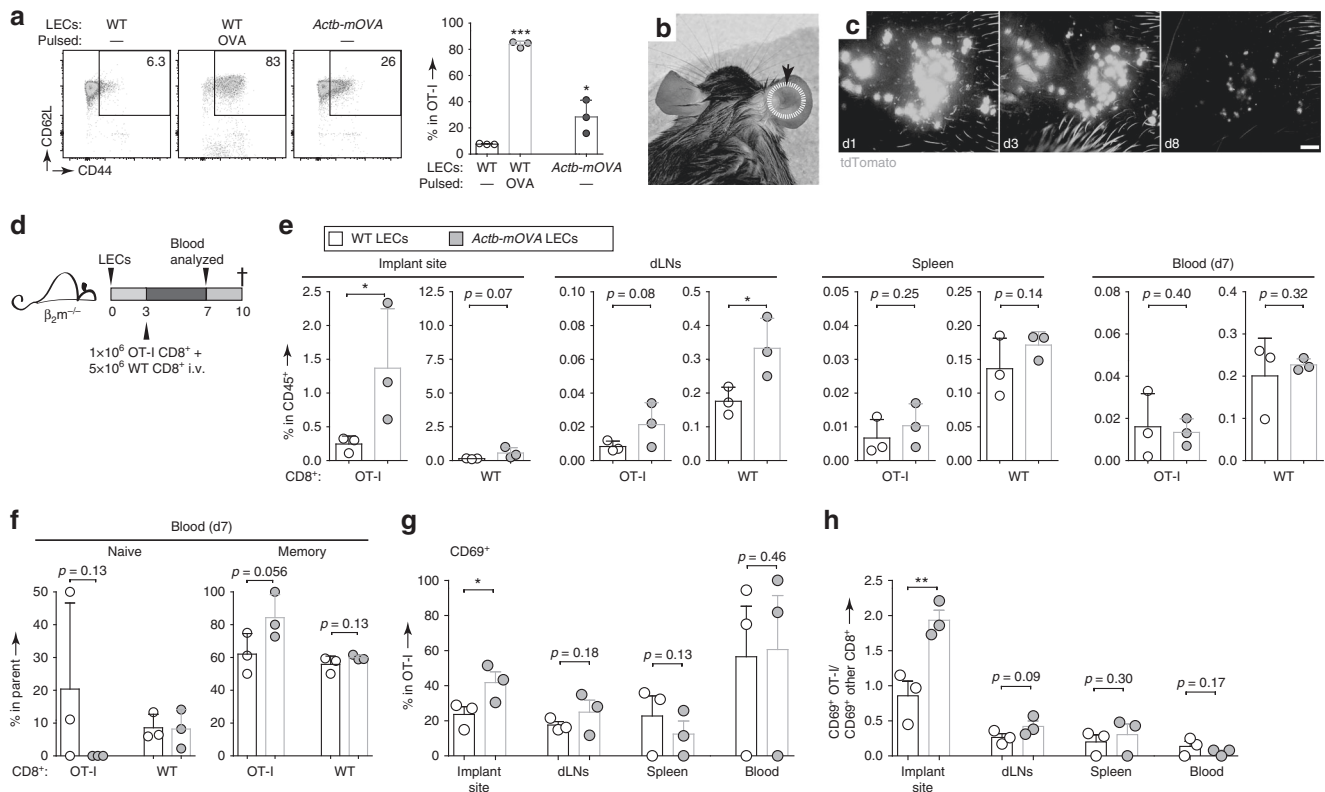


Fig. 3 LECs induce memory phenotype in cognate CD8⁺ T cells in vivo. **a** Memory phenotype of OT-I cells after 3 day co-culture with resting or OVA-pulsed WT primary LN-LECs compared to resting LN-LECs from constitutively OVA-expressing (*Actb-mOVA*) mice (left, representative flow cytometry plots; right, percentages of live OT-I cells with a memory phenotype (CD44⁺CD62L⁺)). **b** Photograph of a mouse that received LEC spheroids in one ear. The implant site is clearly visible for weeks post-implantation due to inflammation (dotted circle). **c** Fluorescent LEC spheroids processed from ProxTom mice after implantation into WT C57Bl/6 mice (scale = 500 μm). **d** Experimental schedule for **e-h**. LECs from WT vs. *Actb-mOVA* mice were processed into spheroids and then implanted into one ear of $\beta_2m^{-/-}$ recipients, which later received 1:5 ratio of cognate (OT-I):bystander (WT) CD8⁺ T cells via the tail vein. Blood (d7) and other organs of interest (d10) were harvested for analysis by flow cytometry. **e** Frequency of OT-I vs. WT CD8⁺ T cells among live immune cells in all organs assayed. Y-axes scales were adjusted to account for the starting ratio of OT-I:WT CD8⁺ T cells. **f** Quantification of percentage of circulating OT-I and bystander CD8⁺ T cells that exhibit naïve (CD44⁻CD62L⁺) versus memory (CD44⁺CD62L⁺) phenotype. **g** Frequency of live OT-I cells that expressed CD69 at all organs assayed. **h** Ratio of activated OT-I cells to activated bystander CD8⁺ T cells, based on CD69 expression at all organs assayed. Columns and error bars indicate mean \pm SD **a, e, f** or SEM **g, h** for $n = 3$ from one representative of two independent experiments.

no differences in the overall numbers of OT-I or bystander CD8⁺ T cells recovered in the blood at 1 week post-transfer (Fig. 3e), there were fewer naïve (CD44⁻CD62L⁺) cells and more memory-like (CD44⁺CD62L⁺) cells among OT-I cells in mice that had received OVA-expressing LECs (Fig. 3f). Moreover, among CD8⁺ T cells isolated from the implant site, mice that received OVA-expressing LECs specifically expanded OT-I cells, and a higher frequency of those OT-I cells expressed CD69 (Fig. 3e, g, h). This increased activation was only seen at the implant site, rather than the superficial cervical LNs draining the implant site (Fig. 3g, h). Together with the data shown in Figs. 1 and 2, these data indicate that antigen presentation by LECs in vivo results in the acquisition of memory phenotype by cognate CD8⁺ T cells.

LECs prime naïve CD8⁺ T cells into T_{CM}/T_{SCM}-like states. To further examine APC-intrinsic differences in the education and activation of cognate CD8⁺ T cells, we turned to in vitro activation studies using CD8⁺ T cells from OT-I mice in co-culture with primary LN LECs or LPS-matured BMDCs (herein referred to as mDC). For antigen, we used a nanoparticle delivery platform for SIINFEKL with a reduction-sensitive linkage, NP-ss-COVA₂₅₀₋₂₆₄ (Fig. 4a-h, Supplementary Fig. 2a-e), which our group has extensively characterized as a tool to detect efficient

cross-presentation^{10,29}. Within 3 days, LEC-educated CD8⁺ T cells proliferated robustly and increased in size compared to naïve cells, indicative of their activated state, although they did not acquire the large blastoid morphology of mDC-educated cells (Fig. 4a, b). Interestingly, we observed that LEC-educated cells primarily expressed a CD44⁺CD62L⁺ phenotype, which was clearly distinct from the effector-like phenotype of mDC-educated cells. This was also distinct from the phenotype of OT-I cells co-cultured with LN FRCs in the presence of OVA₂₅₇₋₂₆₄, which proliferated significantly less than LEC-educated cells and also induced some effector cells (Supplementary Fig. 1). Therefore, OT-I CD8⁺ T cells co-cultured in vitro with LECs, but not with FRCs, acquired a similar phenotype as those educated in vivo in the $\beta_2m^{-/-}$:WT chimeras, further confirming that among the major non-hematopoietic LNSC populations, LECs rather than FRCs promote the acquisition of memory phenotype in CD8⁺ T cells.

We next analyzed the kinetics of T cell phenotype of LEC-educated versus mDC-educated OT-I cells, and we observed that CD62L was initially downregulated on both LEC-educated and mDC-educated cells (Fig. 4b, day 1), consistent with reports that CD62L is cleaved from the cell surface following TCR engagement³⁰. However, as LEC-educated cells proliferated, they predominantly expressed CD62L, whereas the mDC-educated

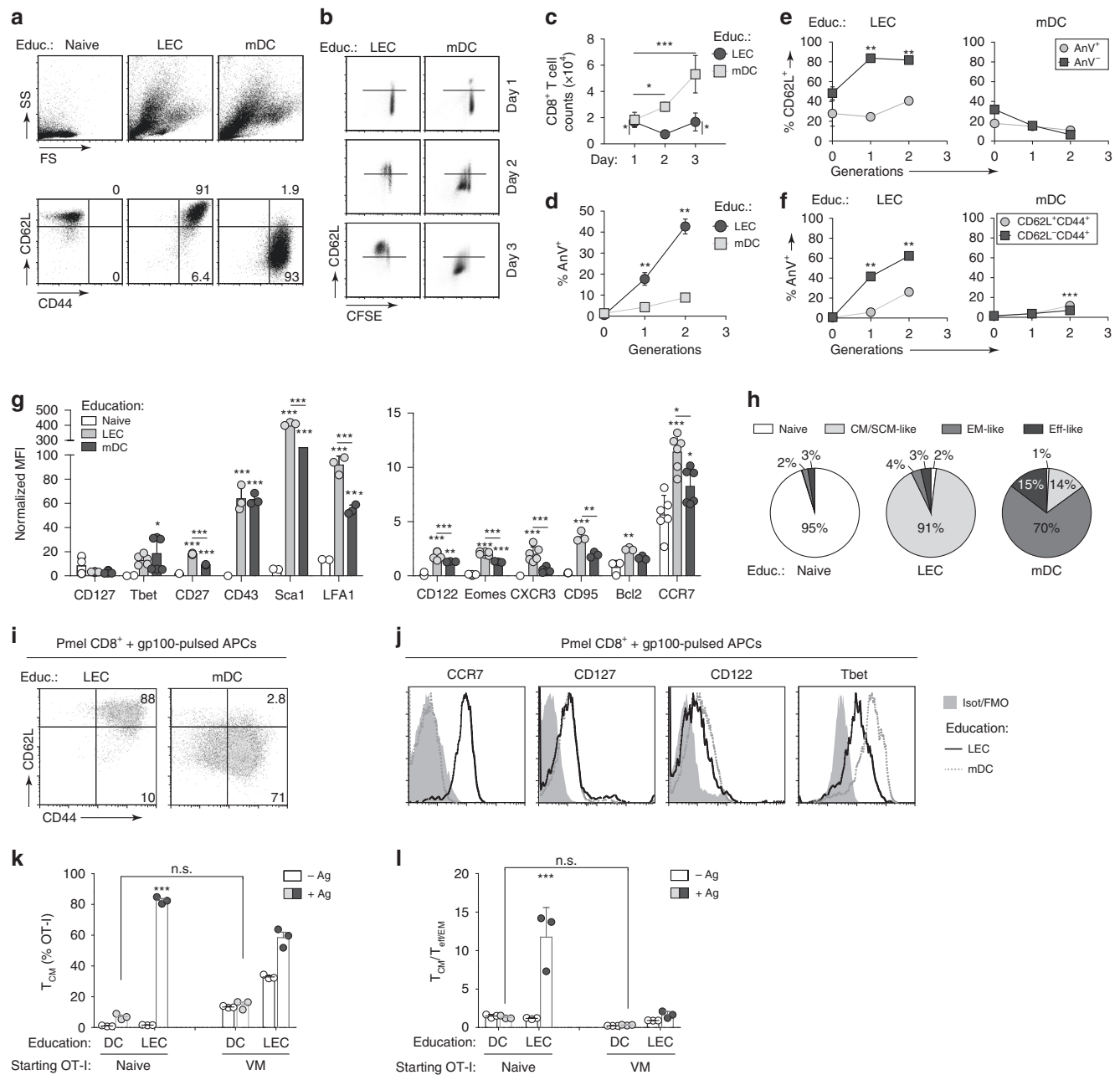


Fig. 4 Surviving LEC-primed CD8⁺ T cells express T_{CM}/T_{SCM}-like phenotype. Flow cytometry analysis of phenotype of naïve CFSE-labeled OT-I cells following 3 days co-culture (unless otherwise noted) with Ag-pulsed LECs or mDCs. As a control, resting naïve OT-I cells have been shown (Educ: Naive). **a** Representative dot plots showing the size and granularity (top) and CD62L and CD44 expression (bottom) of OT-I cells following various co-culture conditions. **b** Representative dot plots of CD62L expression versus CFSE dilution. **c** Absolute recovery of live LEC or mDC-educated cells versus time in co-culture. **d** Percentage of OT-I cells within each generation that stain positive for the apoptotic marker Annexin V (AnV) following 2 days co-culture. **e** Frequency of CD62L⁺ cells per generation gated on AnV⁺ or AnV⁻ OT-I cells, or conversely, **f** AnV⁺ cells gated on the T_{eff/EM}-like (CD44⁺CD62L⁻) or T_{CM}-like (CD44⁺CD62L⁺) cells following 2 days co-culture. **g** Normalized mean fluorescence intensity (MFI); fold-change relative to isotype control for indicated phenotypic markers in CD44⁻CD62L⁺ naïve, versus CD44⁺CD62L⁺ LEC-educated, versus CD44⁺CD62L⁻ mDC-educated cells. **h** Composition of total recovered OT-I cells classified as naïve (CD44⁻CD62L⁺); central memory (CM)-like or stem cell memory (SCM)-like (CD44⁺CD62L⁺CD127⁺CD122⁺Sca1⁺); effector memory (EM)-like (CD44⁺CD62L⁻CD127⁺); effector (Eff)-like (CD44⁺CD62L⁻CD127⁻). **i, j** LECs or mDCs were co-cultured with Pmel CD8⁺ T cells in the presence of gp100₂₅₋₃₃ peptide for 3 days prior to analysis of Pmel phenotype by flow cytometry. Gated on live Pmel CD8⁺ T cells, **i** dot plots indicate expression of CD44 and CD62L, with inset numbers indicating percentages of Pmel cells that occurred within the gate. **j** Histograms depict expression of the indicated phenotypic markers depending on co-culture condition. **k, l** Naïve OT-I cells were sorted by FACS based on CD44 expression as naïve or ‘virtual memory’ (VM) cells prior to 3 days co-cultures. **k** Frequency of T_{CM}-like (CD44⁺CD62L⁺) OT-I cells, **l** ratio of T_{CM}-like to T_{eff/EM}-like (CD44⁺CD62L⁻) cells, both gated on live OT-I cells. Gating strategy in Supplementary Fig. 3b. Data points/columns and error bars indicate mean \pm SD from a representative of two **a-f, k, l** to three **g-j** independent experiments ($n = 3$ technical replicates per experiment); stars indicate significant difference between groups in the same generation **d-f** or compared to naïve group **g**; * $p < 0.05$, ** $p < 0.01$, *** $p \leq 0.001$ by one-way ANOVA **c, g, k, l** or two-way ANOVA **d-f** with Bonferroni post-test.

T cells followed the opposite trend. Moreover, mDC-educated cells expanded continuously, while LEC-educated cell numbers fluctuated over time (Fig. 4c). In agreement with our earlier findings for skin-derived, immortalized LECs¹⁰, a higher fraction of LN LEC-educated T cells were positive for the apoptosis marker AnnexinV (AnV) compared to those educated by mDCs on day 2, when both central and effector memory subsets are detectable (Fig. 4d). However, when we compared the expression of CD62L per generation among AnV⁺ versus AnV⁻ cells, apoptotic LEC-educated OT-I cells were enriched for the CD62L⁻ phenotype, whereas both apoptotic and non-apoptotic mDC-educated cells shared similar frequencies of CD62L⁻ cells (Fig. 4e). Conversely, the T_{eff/EM}-like cells were significantly more apoptotic than the T_{CM}-like cells (Fig. 4f). This observation implies that LEC education induces two divergent populations among CD8⁺ T cells: apoptotic effector-like cells (which are presumably deleted) and surviving predominantly T_{CM}-like cells.

To further investigate the phenotype of LEC-educated T_{CM}-like cells in terms of canonical markers of memory versus effector cell differentiation, we measured a variety of memory-related surface markers using flow cytometry (Fig. 4g, Supplementary Fig. 2a, b). LEC-educated cells expressed CD127 (IL-7R), CD122 (IL-2R β), and CCR7 at levels similar to or higher than in mDC-educated cells. These markers are notable as CD127 and CD122 functionally mediate IL-7 and IL-15-mediated signaling for the homeostatic proliferation of memory cells, while CCR7 allows homing of T_{CM} cells to secondary lymphoid organs³¹. Furthermore, the relative expression in LEC-educated T cells of the transcription factors (TFs) Eomes and Tbet (*Tbx21*), which are mutual antagonists that counter-regulate memory vs. effector differentiation³², was consistent with a T_{CM}-like phenotype (increasing Eomes and decreasing Tbet) (Fig. 4g, Supplementary Fig. 2b). Interestingly, LEC-educated cells expressed additional markers that may delineate a subset of stem cell-like memory T cells (T_{SCM})^{33–35}, including stronger expression of Sca1, B cell lymphoma 2 (*Bcl2*), CD27, CD95 (*Fas*), CXCR3, and LFA1 compared to mDC-educated cells.

Further illustrating phenotypic differences between LEC-educated and mDC-educated CD8⁺ T cells (Fig. 4h), most LEC-educated cells were CD44⁺CD62L⁺ (T_{CM/SCM}-like) with the largest subset expressing high levels of CD127, CD122, and Sca1, whereas mDC-educated cells were mostly CD44⁺CD62L⁻CD127⁺ (T_{eff/EM}-like). We further observed a distinct cytokine milieu in LEC- versus mDC-CD8⁺ T cell co-cultures (Supplementary Fig. 2c), with increased G-CSF, eotaxin (CCL11), CXCL1, CXCL10, CCL7, IL-31, CCL2, and CXCL2, and decreased IFN γ , IL-13, IL-17, IL-2, IL-22, TNF α , GM-CSF, and RANKL. In both LEC and mDC co-cultures with OT-I cells, IL-7 and IL-15, which are known to contribute to the induction of T_{SCM} cells³⁶, were similarly present, but at the mRNA level, LEC expression of these cytokines were increased upon cognate T cell activation (Supplementary Fig. 2d, e).

LEC-educated CD8⁺ T cells similarly acquired memory characteristics regardless of whether we used free or nanoparticle-bound SIINFEKL peptide (NP-ss-COVA₂₅₀₋₂₆₄) or full-length ovalbumin (Fig. 3a, Supplementary Figs. 1, 2f). We also examined if TCR affinity may affect memory phenotype acquisition by adapting the co-culture experiments to naïve OT-3 CD8⁺ T cells, which possess TCRs with a lower affinity for the SIINFEKL peptide than OT-I CD8⁺ T cells³⁷. TCR affinity accounted for a reduction in the overall frequency of activated OT-3 cells (~50% when educated by LECs and ~80% by mDCs compared to ~98% of OT-I cells for both education conditions). Nonetheless, OT-3 cells preferentially acquired a memory phenotype when educated by LECs (Supplementary Fig. 2g). Importantly, these same observations also held true in other

antigen-transgenic TCR systems, such as with Pmel CD8⁺ T cells co-cultured with gp100 peptide-pulsed LECs (Fig. 4i, j).

Because naïve OT-I mice often harbor a significant population of CD44⁺ CD8⁺ T cells, or so-called ‘virtual memory’ (VM) cells³⁸, we wanted to rule out the possibility that the activated phenotype we saw in LEC-educated OT-I cells in these studies was not due to those cells being re-activated, rather than from priming of naïve cells. To this end, we sorted OT-I splenocytes based on naïve (CD44⁻CD62L⁺) or VM phenotype (CD44⁺) prior to co-culture with LECs or mDCs pre-pulsed with full-length OVA protein (Fig. 4k, l, Supplementary Fig. 3). We found that >80% of LEC-educated naïve OT-I cells acquired a CD44⁺CD62L⁺ phenotype, compared to ~57% for LEC-reactivated ‘VM’ OT-I cells (Fig. 4k, l, Supplementary Fig. 3b). This correlated with increased IL-2 production (Supplementary Fig. 3c), further confirming the T_{CM}-like phenotype of these cells.

Collectively, these data indicate that LEC-educated CD8⁺ T cells phenotypically show characteristics of both T_{CM} and T_{SCM} subsets, independently of the transgenic TCR tested (i.e., CD8⁺ T cells from OT-I, OT-3, and Pmel mice) or the antigen formulation (peptide, full-length protein, or nanoparticle-bound), and are distinct from the T_{eff/EM}-like phenotype acquired by DC-educated cells under inflammatory conditions.

LEC-primed CD8⁺ T cells express a memory-like transcriptome. To determine whether the phenotypic differences we saw between LEC-educated and mDC-educated T cells are reflected at the transcriptomic level, we performed RNA sequencing to characterize and quantify the transcriptional profiles of naïve, LEC-educated and mDC-educated CD8⁺ T cells after up to 3 days of co-culture. Unsupervised principal component analysis (PCA) (Fig. 5a) and hierarchical clustering (Supplementary Fig. 4a) were performed to visualize the kinetics of T_{CM}-like and T_{EM}-like phenotype acquisition by LEC-educated and mDC-educated CD8⁺ T cells, respectively, and to potentially identify sets of genes that were modulated by differences in the APCs across time. The first and second principal components (PC1 and PC2) explained ~52% and 18%, respectively, of the total variance in gene expression profiles. Interestingly, while LEC and mDC-educated cells clustered closely to one another on day 1, both shifted along the PC2 axis over the 3 days co-culture period, with LEC-educated cells diverging on the last day from mDC-educated cells along the PC1 axis toward naïve cells (Fig. 5a). Therefore, we reasoned that PC1 is likely to primarily contain genes that differentiate antigen-experienced from naïve T cells, while PC2 likely accounted for genes associated with memory/effector differentiation.

Focusing solely on the expression of memory/effector signature genes, we saw that LEC-educated cells (Fig. 5b, Supplementary Fig. 4b) displayed higher expression of genes related with the T_{CM}/T_{SCM} subsets (*Sell*, *Cd27*, *Cd28*, *Ly6e*, *Ccr7*) by d3, whereas mDC-educated cells expressed higher levels of genes consistent with an effector signature (*Gzm*'s, *Prf1*, *Ifng*, *Il2ra*, *Cxcr5*, *Sema7a*), with the exception of *Pdcd1* (encoding PD-1), which was highly upregulated in LEC-educated cells as previously reported¹⁰. Notably, *Sell* (CD62L) expression was initially downregulated in LEC-educated cells on day 1, but then upregulated to levels similar to those in naïve cells, consistent with our observations at the protein level (Fig. 4b). This trend was also observed in LEC-educated cells for other memory-associated genes (*Cd27*, *Cd28*, *Ly6e*, *Spn*, *Il7r*, and *Ccr7*), while mDC-educated cells either failed to upregulate or upregulated them to a lesser extent (Fig. 5b, c, Supplementary Fig. 4b). Finally, consistent with our observations that some LEC-educated cells

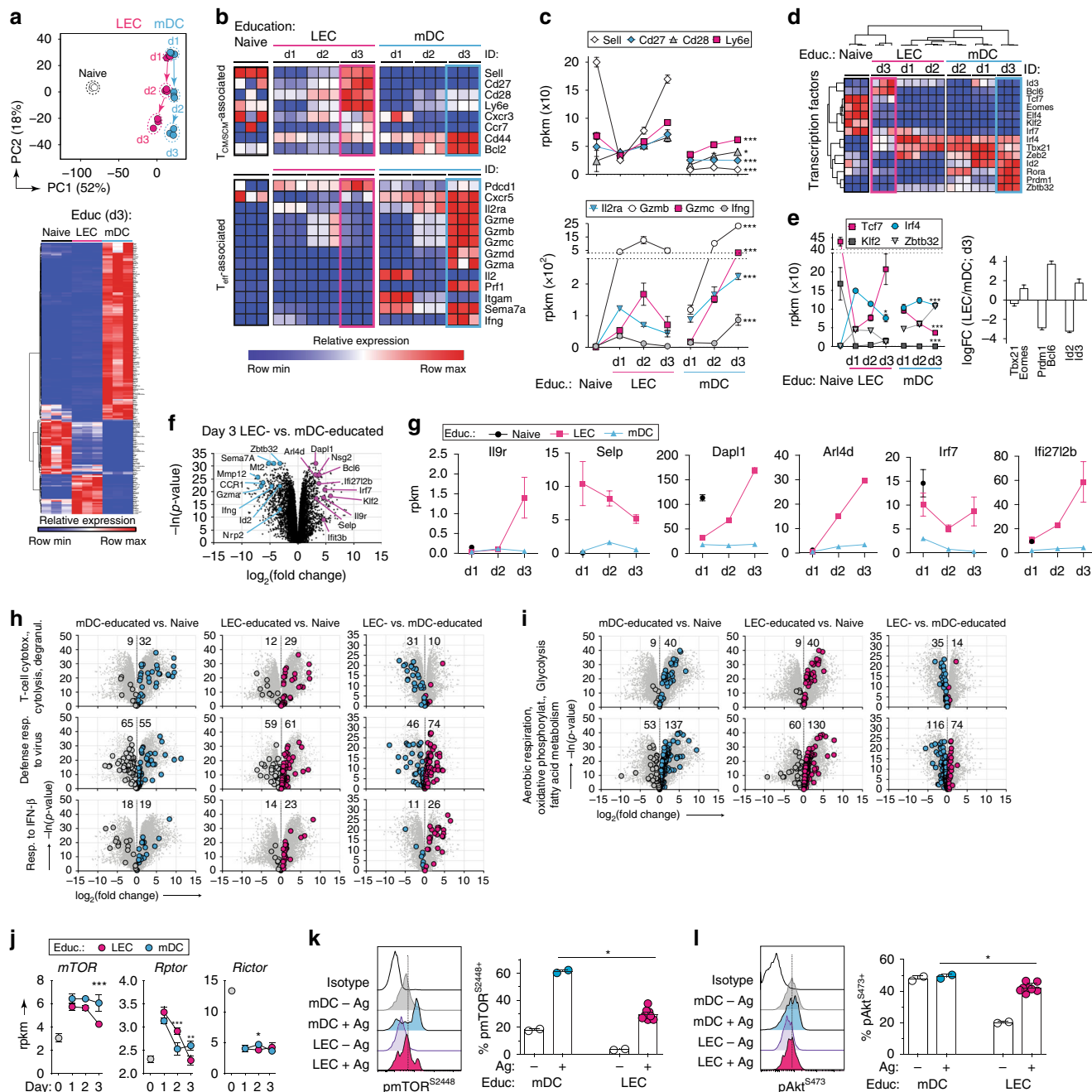


Fig. 5 Transcriptome and metabolic signaling in LEC-educated CD8⁺ T cells is consistent with T_{CM}/T_{SCM}-like phenotype. Naïve OT-I cells were educated in the presence of antigen by LECs or mDCs for up to 3 days and subsequently analyzed by RNA sequencing. Resting naïve OT-I cells have been shown for comparison. **a** (top) Principal component analysis (PCA) of most-modulated genes across time and APC type suggest PC1 (52% of variance) includes genes related to antigen experience and APC type, whereas PC2 (18% of variance) contains genes related to the effects of time. (bottom) Heatmap depicting the most significant differences in gene profiles following 3 days of education by LECs or mDC, filtering for changes in expression ($|\log_2FC| > 2.89$) between mDC/LEC-educated CD8⁺ T cells and $p < 0.01$. **b** Heat maps depicting normalized expression levels of various memory-associated and effector-associated genes on OT-I cells according to co-culture condition and time. Each column represents data originating from a single biological replicate. **c** Normalized expression (rpkm; reads per kilobase per million mapped reads) of selected genes over time, comparing effects of LEC vs. mDC education. **d** Unsupervised hierarchical clustering analysis to identify dynamics of gene expression encoding TFs regulating effector/memory differentiation. **e** (left) Normalized expression of genes encoding TFs related with memory (*Tcf7*, *Klf2*) versus effector (*Irf4*, *Zbtb32*) differentiation. (right) Log fold-change in expression of indicated transcription factors due to LEC education, relative to mDC education. $p < 0.001$ for all except *Tbx21* ($p < 0.01$). **f** Volcano plot highlighting most-modulated genes following LEC education (magenta) or mDC education (blue), and **g** kinetics of normalized expression of selected genes. **h**, **i** Pairwise-comparison of transcriptomes as volcano plots highlighting sets of genes linked to specific biological processes, as annotated on the Gene Ontology Atlas⁴⁷. **i** Volcano plots for genes associated with anabolic (glycolysis) and catabolic processes (oxidative phosphorylation, aerobic respiration, and fatty acid oxidation). **j** Normalized gene expression (rpkm) of genes encoding the central mediators of the mTOR-signaling pathway, including components of the mTORC1 (*Raptor*) or mTORC2 (*Rictor*) complexes. **k**, **l** SIINFEKL-pulsed LECs or mDCs were co-cultured with naïve OT-I cells for 2 h in vitro, and phosphorylated **k** mTOR^{S2448} and **l** Akt^{S473} was quantified on OT-I by intracellular flow cytometry. Data points and error bars indicate mean \pm SD of $n = 3$ biological replicates **a–j** or $n = 2–8$ technical replicates **k**, **l**. $*p \leq 0.05$, $**p \leq 0.01$, $***p \leq 0.001$ via one-way ANOVA with Benjamini–Hochberg correction for false discovery rate (FDR).

differentiate into apoptotic effectors, we saw some genes related to effector function (*Il2ra*, *Gzmb*, *Gzmc*, *Ifng*) upregulated at d1, but expression dropped drastically by d3.

T cell differentiation and functionality are regulated by the tightly tuned expression of several TFs^{11,32,39}, and over 3 days in co-culture LEC-educated T cells expressed increasing levels of genes encoding TFs favoring long-term survival and proliferative potential (e.g., *Id3*, *Bcl6*, *Tcf7*, *Eomes*, *Elf4*, *Klf2*, and *Irf7*), and low levels of TFs associated with effector differentiation (e.g., *Irf4*, *Zbtb32*, *Tbx21*, *Zeb2*, *Id2*, *Rora*, *Prdm1*). In contrast, mDC-educated cells exhibited the opposite trends (Fig. 5d, e, Supplementary Fig. 4c). This divergence appeared most pronounced at d3, when LEC-educated and mDC-educated cells displayed diametrically opposed expression patterns for genes encoding TFs known to act in mutually antagonistic pairs (*Eomes-Tbx21*, *Bcl6-Prdm1*, *Id3-Id2*) to coordinate memory versus effector differentiation, respectively³² (Fig. 5e). Moreover, d3 LEC-educated T cells clustered closer to naïve T cells than to mDC-educated T cells by hierarchical clustering analysis (Fig. 5c), supporting their relatedness to resting cells with the potential for long-term survival.

To identify the unique gene expression signature in LEC-educated cells, we filtered our dataset for genes that were most differentially regulated (mean $|\log_2FC| \geq 2.89$ and $p < 0.01$) between day 3 LEC-educated versus mDC-educated cells, arriving at a subset of ~200 genes (Fig. 5f, Supplementary Table 1). Among the genes that mDC-educated cells upregulated the most were those associated with T cell activation and effector potential (*Sema7a*, *Ccr1*, *Nrp2*, *Zbtb32*, *Prdm1*, *Id2*) and effector function (*Ifng*, *Gzma*, *Gzmd*, *Gzmg*, *Gzmf*). In contrast, the most differentially expressed genes in LEC-educated cells were correlated with the T_{CM} -specific signature, including *Bcl6*, a key signal for memory T cell differentiation⁴⁰; *Dapl1*, overexpressed in early memory cells⁴¹; and the small GTPase *Arl4d*, linked with limited early-effector CD8⁺ T cell development upon viral infection⁴² (Fig. 5g). Additionally, LEC-educated OT-I cells also expressed signatures of pharmacologically induced T_{SCM} cells⁴³ including interferon-responsive genes (*Ifi2712a*, *Ifi2712b*, *Ifit1*, *Ifit3*, *Ifit3b*), *Selp* and *Isg15* (all important for antiviral innate immunity), *Irf7* and *Il9r*; members of the tripartite motif-containing protein 30 (*Trim30*) family—which fine-tune the threshold to effector function⁴⁴; as well as *Klf2*—which can activate and maintain CD62L and CCR7 expressions⁴⁵. Surprisingly, LEC-educated cells also upregulated several neuron-related genes, such as *Cnr2*, *Slfm5*, and *Nsg2* (Supplementary Fig. 4d), which, together with *Sell* and *Xcl1*, comprise a gene expression pattern of naïve and late memory T cells⁴⁶. In addition, a number of genes previously identified as differentially expressed between T_{SCM} and T_{CM} cells³³ were also expressed at higher levels in LEC-educated cells (Supplementary Fig. 4e).

LEC priming preferentially engages memory-related pathways.

We next made use of genome-wide functional annotations provided by the Gene Ontology Consortium⁴⁷ and mapped genes corresponding to specific biological functions onto volcano plots comparing naïve, LEC-educated or mDC-educated cells (Fig. 5h, i and Supplementary Fig. 4f). Although both LEC/mDC-educated cells upregulated genes related to T cell cytotoxicity relative to naïve OT-I cells, mDC-educated cells upregulated them to a much greater extent, highlighting the limited effector function of LEC-educated cells. On the other hand, LEC-educated cells upregulated genes associated with response to IFN β and defense response to viral infections (Fig. 5h).

Since metabolism and T cell differentiation state are inter-related processes⁴⁸, we examined the expression of genes related to respiratory chain and fatty-acid metabolic programs, typically associated with resting naïve and memory T cells, and glycolysis, which is dominant in proliferating effector cells (Fig. 5i). Both LEC/mDC-educated cells upregulated genes related to these metabolic programs compared to naïve cells, while glycolysis-associated genes were more upregulated in mDC-educated cells, confirming that LEC-educated cells are less prone to effector differentiation.

Crucially implicated in the regulation of these metabolic processes is the mammalian target of rapamycin (mTOR) pathway, which integrates intracellular and extracellular signals, leading to the formation of either of two multiprotein complexes, mTORC1 or mTORC2, which propagate different downstream signals. Blockade of mTORC1 was shown to favor memory T cell generation⁴⁹ and induce T_{SCM} differentiation⁴³, while suppression of mTORC2 activity enhanced memory CD8⁺ T cell formation⁵⁰. We detected consistently lower levels of *mTOR* in LEC-educated compared to mDC-educated cells at all time points examined (Fig. 5j, Supplementary Fig. 4g). Furthermore, while they both expressed similar levels of *Rictor*, LEC-educated cells displayed significantly lower *Rptor* expression on d3, suggesting a lower induction of the mTORC1 complex. To further confirm these observations at the protein level, we assessed the phosphorylation of mTOR (pmTOR^{S2448}) and Akt (pAkt^{S473}, indicative of mTORC2 activity) by flow cytometry (Fig. 5k, l). Within 2 h of co-culture, mDC education was superior to LEC education in inducing pmTOR^{S2448+} and pAkt^{S473+} in OT-I cells, suggesting that both mTORC1 and mTORC2 were indeed less active and that PI3K–Akt–mTOR activity is less sustained in LEC-educated cells.

Altogether, these data validate the T_{CM}/T_{SCM} -like phenotypic properties of LEC-educated CD8⁺ T cells, which exhibit transcriptional and metabolic programs consistent with a memory-like differentiation state, distinct from mDC-educated cells.

In vitro LEC-primed CD8⁺ T cells have memory-like LN-homing.

The elevated expression levels of CD62L in LEC-educated cells prompted us to investigate whether they exhibit preferential migration to secondary lymphoid organs, because CD62L enables naïve and T_{CM} cells to localize to lymphoid tissue⁵¹. To this end, we transferred naïve or LEC/mDC-educated OT-I cells into mice and analyzed their homing into various organs 1 week later (Fig. 6a). LEC-educated cells homed primarily to secondary lymphoid organs (LN and spleen, 53%) whereas mDC-educated cells migrated mainly to the periphery (lungs and liver, 67%) (Fig. 6b). A smaller fraction of mDC-educated cells was found in lymphoid tissues (33%), to which naïve cells almost exclusively homed (91%), as expected.

LEC-educated cells that homed to the LNs and spleen primarily expressed a T_{CM} -like (CD44⁺CD62L⁺) phenotype (Fig. 6c, d), as well as in the rest of the organs examined (Supplementary Fig. 5a). In contrast, mDC-educated cells were predominantly $T_{eff/EM}$ -like (CD44⁺CD62L⁻) in all organs except in the LN, where they were mostly T_{CM} . LEC-educated cells possessed a higher ratio of $T_{CM}/T_{eff/EM}$ than mDC-educated cells in all organs examined, with the highest ratio in the LN, while for mDC-educated cells, the ratio $T_{CM}/T_{eff/EM}$ was <1 in all organs except in the LN, underlining the phenotypic divergence due to their education (Fig. 6e, Supplementary Fig. 5b, c).

To determine whether LEC-educated cells preferentially localized to specific sub-anatomic sites in the LN, we co-transferred LEC-educated and naïve CD8⁺ T cells, each labeled

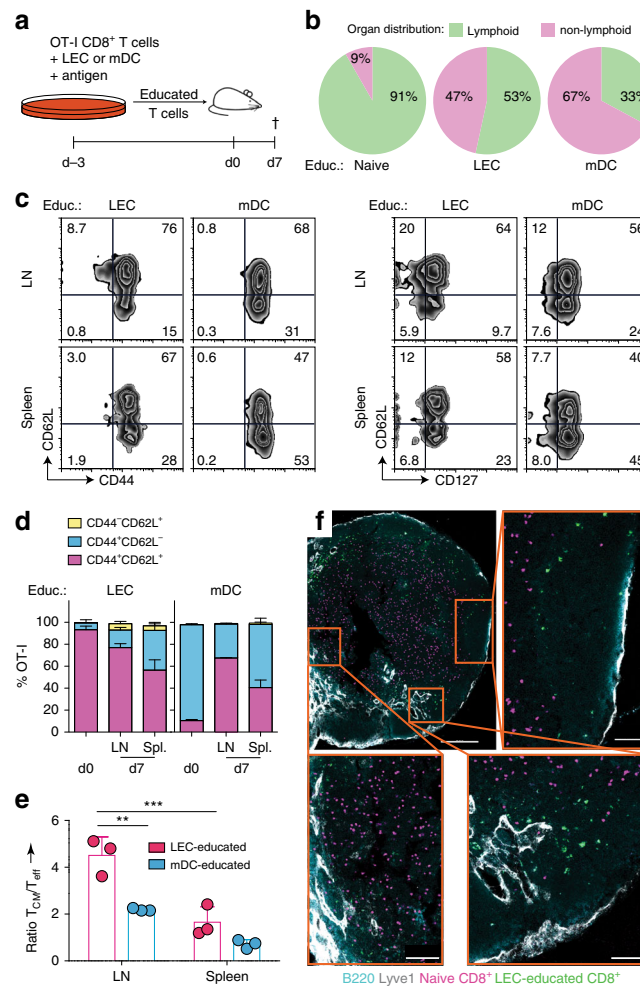


Fig. 6 CD62L expression in LEC-educated CD8⁺ T cells correlates with LN homing after in vivo transfer. **a** LEC-educated or mDC-educated CD45.1⁺ OT-I cells were transferred i.v. into healthy adult WT mice (10⁶ cells/recipient), and various organs were analyzed one week later. **b** Recovered transferred cells within either lymphoid (LN, spleen) or non-lymphoid (liver and lungs) organs as a percentage of total recovered cells across these organs. **c** Representative flow cytometry contour plots depicting expression of CD44, CD62L, and CD127 gated on OT-I cells. **d** Distribution of T_{CM}-like (CD44⁺CD62L⁺), T_{eff/EM}-like (CD44⁺CD62L⁻) and naïve (CD44⁻CD62L⁺) subsets within LEC/mDC-educated cells before transfer (day 0) and at endpoint. **e** Ratio of T_{CM}-like to T_{eff/EM}-like cells. Data points and error bars indicate mean ± SD for *n* = 3 biological replicates from one of two independent experiments. ***p* ≤ 0.01, ****p* ≤ 0.001 via two-way ANOVA with Bonferroni's post-test. **f** Top left, brachial LNs collected from healthy wild-type mice within 2 days after co-transfer of LEC-educated (green) and naïve (pink) OT-I cells were analyzed by imaging, with counterstains for Lyve1 (white) and B220 (cyan) for orientation. Overview wide-angle and close-ups of (top and bottom right) subcapsular sinus and B cell zones, and (bottom left) T cell zone. Scale = 200 μm (top left), 70 μm (bottom left), and 50 μm (top/bottom right). Representative image from two independent experiments.

with different fluorophores, and after a week, imaged thick sections of the brachial LN using confocal microscopy. We observed the naïve cells primarily in the paracortical T cell zone (Fig. 6f), while the LEC-educated cells localized mostly near the cortical and medullary sinuses, around B cell follicles and particularly in the interfollicular areas. These homing patterns are consistent with recent descriptions for naïve and memory CD8⁺ T cells^{52,53}.

Collectively, these data suggest that CD62L expression in LEC-educated cells is functional and corresponds to preferential migration to secondary lymphoid organs.

Re-stimulation of LEC-educated CD8⁺ T_{CM} generates cytotoxic lymphocytes. The most important function of memory T cells is their reactivation potential, so we next assessed their response to a secondary challenge. To model this process in vitro, OT-I cells were educated by LECs or mDCs for 3 days, after which they were CFSE-labeled and further co-cultured with

mDCs loaded with SIINFEKL (mDC-recall, +Ag) or without antigen (-Ag) (Fig. 7a). After 24 h, we uniquely detected low levels of proliferation upon antigen recall in LEC-educated cells (Fig. 7b, Supplementary Fig. 6a), consistent with the proliferation potential of T_{CM} cells. More importantly, reactivated LEC-educated cells exited their non-responsive state and produced even higher levels of TNFα and IL-2 compared to mDC-educated cells (Fig. 7c, Supplementary Fig. 6b), and acquired more of an effector-like phenotype with downregulation of CD62L and increased expression of granzyme-B (GzB) (Fig. 7d-f), although not to the same extent as mDC-educated cells.

Because LEC-educated cells responded to an in vitro antigen recall with a strong, multifunctional response, we asked whether this translates to rapid recall responses following secondary challenge under inflammatory conditions in vivo. For this purpose, we transferred CFSE-labeled LEC-educated or mDC-educated OT-I cells into mice, and after 5 days, we administered OVA with LPS (+RECALL) or saline (-RECALL) s.c. (Fig. 7g). Both LEC-educated and mDC-educated CD8⁺ T cells (which

may have been induced to divide at different rates before the time of CFSE labeling) expanded significantly within the LNs and spleens of recalled recipients, even to the point of completely diluting CFSE before the endpoint (Fig. 7h, i). Based on cell recovery, compared to non-recalled recipients, recalled LEC-educated T cell numbers increased four-fold in the LN and the spleen, while recalled mDC-educated cells increased 0.5-fold.

This surprising difference may be attributable to the tendency of LEC-educated T cells to be enriched in memory-like cells, which in theory, possess superior expansion potential than the effector-like cells generated by mDC education. Additionally, LEC-educated cells were particularly enriched in the LN compared to the spleen, a result attributable to the early time point following challenge and their homing properties (Fig. 6). Along with the vigorous expansion, and in agreement with our *in vitro* observations, LEC-educated cells also exhibited the functional potential expected of memory cells by upregulating effector cytokines (Fig. 7j, k). Following *ex vivo* re-stimulation, we noted increased production of IFN γ and TNF α in antigen-recalled mice, and furthermore, the transferred cells acquired effector function, expressing GzB and demonstrating cytolytic capacity (Fig. 7l), although mDC-educated CD8⁺ T cells were superior by all measures.

Because true memory cells persist even in the absence of antigen, we repeated the above experiment but with re-challenge after >5 weeks of LEC-educated or mDC-educated OT-I cell transfer (Fig. 7g, long-term recall). Both LEC-educated and mDC-educated T cells expanded following recall (Fig. 7m), with LEC-educated cells giving rise to effector-like cells in both the LN and spleen (Fig. 7n, o), though to a less extent than mDC-educated T cells. Similar frequencies of LEC-educated and mDC-educated cells acquired the short-lived effector phenotype (KLRG1⁺CD127⁻), which was predominantly expressed by OT-I cells in the spleen, especially by mDC-educated cells (Fig. 7o). Overall, the phenotypes of LEC-educated T cells resembled those of mDC-educated cells, although LEC-educated cells achieved significantly lower frequencies of T_{eff/EM} (CD44⁺CD62L⁻) cells (Fig. 7o, Supplementary Fig. 6c). The differences seen in the magnitude of responses in LEC-educated vs. DC-educated T cells upon recall are likely due to differences in their phenotypes and degree of activation at the time of adoptive transfer.

Taken together, these data suggest that LEC-educated CD8⁺ memory-like T cells can acquire cytotoxic function and effector phenotype upon antigen re-encounter. The ability of antigen-experienced T cells to proliferate and differentiate into cytotoxic lymphocytes upon secondary challenge constitutes a hallmark of immunological memory, adapted to long-term immune protection in the host.

LEC-educated CD8⁺ T cell memory protects against infection.

These findings raised the question of whether LEC-educated CD8⁺ T cells can mediate protective immunity against a pathogen in a manner comparable to mDC-educated cells. To first measure the cellular response to memory recall, we co-transferred LEC-educated (CD45.1/2⁺) and mDC-educated (CD45.1⁺) OT-I cells (1:1) in mice and after 5 weeks, challenged the mice with OVA-expressing *Listeria monocytogenes* (*L.m.*-OVA) (Fig. 8a). Within a week post-infection, LEC-educated cells expanded from making up 0.5 ± 0.4% of all circulating CD8⁺ T cells to 11.2 ± 5.0%, and mDC-educated cells further expanded by at least two-fold (Fig. 8b, c). These trends were not observed in the dLNs (Supplementary Fig. 7a), due to the systemic route of *L.m.*-OVA infection.

Importantly, LEC-educated cells acquired effector function to a similar extent as mDC-educated cells upon *ex vivo* re-stimulation, exhibiting comparable cytotoxic potential as demonstrated

through the frequency of cells producing effector cytokines (IFN γ , TNF α , IL-2) and expressing CD107a, which signifies cytolytic granule release (Fig. 8d, e, Supplementary Fig. 7b). Interestingly, LEC-educated cells trended towards higher polyfunctionality than DC-educated cells, defined as double or triple positive for IFN γ , TNF α , and IL-2 ($p = 0.07$; Fig. 8f, Supplementary Fig. 7c).

Consistent with our previous observations, LEC-educated cells acquired a predominantly effector phenotype (CD44⁺CD62L⁻) by d8 post-infection (Fig. 8g, h), and most were found within the KLRG1⁺CD127⁻ subset. Remarkably, we also observed a significant T_{CM}-like (CD44⁺CD62L⁺) subset among LEC-educated cells, which led to a significantly larger T_{CM}/T_{eff/EM} ratio relative to mDC-educated cells (Fig. 8h). We additionally noted a significantly higher ratio of memory precursors (KLRG1⁻CD127⁺) to short-lived effectors within the LEC-educated population in both the spleen and LN (Supplementary Fig. 7d).

To directly compare the protective functions of LEC-educated versus mDC-educated cells, we injected mice with either LEC-educated or mDC-educated cells (Fig. 8a, bottom branch). In comparison to mice that received resting CD8⁺ T cells (Educ: Naïve), LEC-educated CD8⁺ T cells and mDC-educated T cells were similarly competent at controlling the bacterial load following infection with *L.m.*-OVA (Fig. 8i).

We also noted that LEC-educated T cells uniquely retained a population of T_{CM}-like phenotype following antigen re-encounter (Fig. 7d, n) or pathogenic infection (Fig. 8g, h), so we asked whether LEC-educated cells were preferentially capable of generating a secondary T_{CM}-like subset. We co-transferred LEC-/mDC-educated OT-I cells (Fig. 8a, top branch) and tracked the transferred cells for 2 weeks post-infection. While the cytotoxic effector fraction (CD44⁺GzB⁺) decreased over time in both groups, only the LEC-educated cells showed a concomitant and significant increase in the T_{CM}-like phenotype within 9 days post-infection (Fig. 8j, Supplementary Fig. 7e). Furthermore, 3 weeks post-infection, LEC-educated cells possessed a higher ratio of CD127⁺CD62L⁺ to CD127⁺CD62L⁻ cells in the spleen and LN (Fig. 8k). Additionally, we observed similar trends for the T_{CM}/T_{eff/EM} and the memory precursor-to-short-lived effector ratios in both organs (Supplementary Fig. 7f). Finally, the frequency of CD44⁺CD62L⁺CD122⁺ cells was significantly higher among LEC-educated cells in both the LN and spleen.

We followed up with an evaluation of LEC-educated T_{CM} responses to homeostatic signals *in vitro* (Supplementary Fig. 8a). Similar to conventional T_{CM}/T_{SCM} cells³³, LEC-educated cells underwent homeostatic turnover and displayed increased survival in response to IL-15 compared to mDC-educated cells (Supplementary Fig. 8b). Notably, LEC-educated cells retained their initial CD44⁺CD62L⁺ phenotype following IL-15-dependent proliferation (Supplementary Fig. 8c), suggesting self-renewal capacity.

Overall, our findings indicate that LEC-educated CD8⁺ T_{CM}/T_{SCM} cells can be reactivated to participate in protective immunity while also possessing the capacity for self-renewal, giving rise to a persistent secondary-memory population.

Requirements for LEC-educated CD8⁺ T_{CM} polyfunctionality.

Finally, we sought to identify the signals that may lead to functional re-activation of LEC-educated CD8⁺ T cells. To evaluate the roles of TCR stimulation and co-stimulation, LEC-educated OT-I cells were treated with α CD3 with or without α CD28 (Fig. 9a). TCR ligation by α CD3 was sufficient to induce IFN γ production; but co-stimulation through α CD28 was required to induce polyfunctional cells (Fig. 9b).

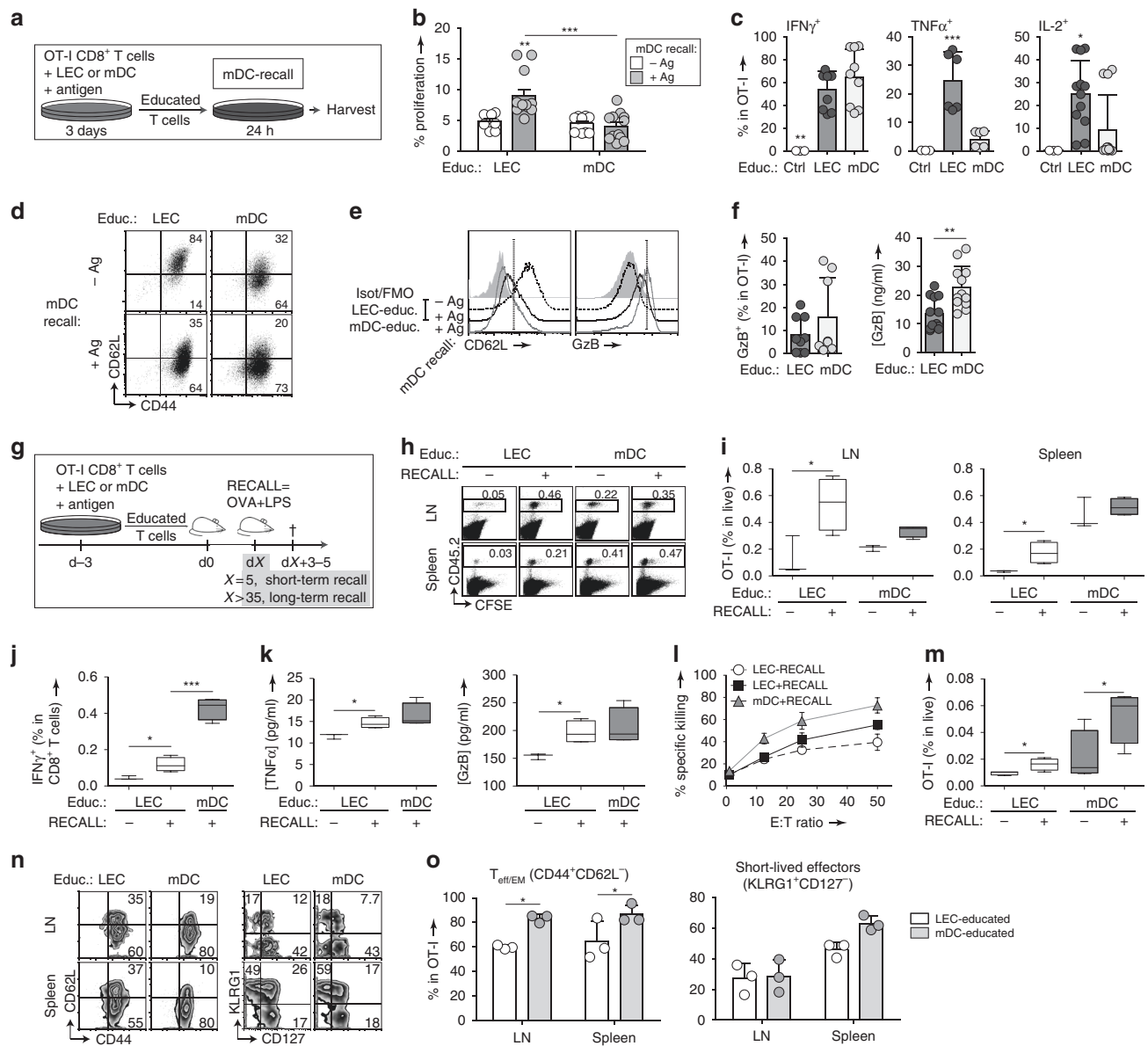


Fig. 7 LEC-educated CD8⁺ T cells expand rapidly and differentiate into effector cells upon secondary challenge. **a** Experimental setup for **b–f**: CFSE-labeled LEC/mDC-educated cells were recalled with Ag-pulsed or control mDCs. **b** Percentage of CD8⁺ T cells that were proliferating at endpoint. **c** Frequency of IFN γ ⁺, TNF α ⁺, and IL-2⁺ cells among live OT-I cells. **d** Representative dot plots depicting CD62L and CD44 expression gated on OT-I cells depending on initial education conditions and antigen recall, and **e** according histograms depicting CD62L and GzB expression. **f** Frequency of intracellular GzB⁺ OT-I cells and production of GzB detected by ELISA in cell culture supernatants. **g** Experimental setup for **h–o**: CFSE-labeled CD45.2⁺ LEC/mDC-educated OT-I cells were transferred into CD45.1⁺ wild-type adult mice, and recalled with OVA/LPS at the short-term (5 days post-transfer, **h–i**) or long-term (>5 weeks post-transfer, **m–o**) memory phases. As a negative control, some recipients received a mock buffer injection (RECALL: –). **h** CFSE dilution on transferred cells recovered from LNs or spleens. **i** Composition of transferred cells among all live cells in the LNs or spleen. **j** Frequency of intracellular IFN γ ⁺ cells among transferred cells. **k** Endpoint concentrations of TNF α and GzB production after ex vivo re-stimulation. **l** Cytotoxicity of recalled LEC-educated vs. mDC-educated OT-I cells measured based on specific killing of antigen-pulsed target cells relative to non-specific killing of scrambled peptide-pulsed target cells. E:T = effector to target cell ratio. **m** Composition of OT-I cells among live cells in the LNs after long-term recall. **n** Representative flow cytometry plots depicting expression of CD44, CD62L, CD127, and KLRG1 gated on OT-I cells. **o** Frequency of T_{eff/EM} (CD44⁺CD62L[–]) and short-lived effectors (KLRG1⁺CD127[–]) within OT-I cells. Data points and error bars indicate mean \pm SD for $n = 3–7$ biological replicates pooled from up to three independent experiments. Whiskers: Min to Max, median **i–k, m**. * $p \leq 0.05$, ** $p \leq 0.01$, *** $p \leq 0.001$ by two-way ANOVA **b, l, o**, one-way ANOVA with Bonferroni's post-test **c**, or by two-tailed unpaired Student's *t*-test **f, i–k, m**.

To ask if undesirable reactivation of LEC-educated cells could be triggered under homeostatic conditions, we examined their functional profile following reactivation with immature DCs (iDCs) in the presence of immunogenic or immunosuppressive signals. LEC-educated or mDC-educated OT-I cells were cultured together with iDCs (iDC-recall), with or without SIINFEKL,

either in the presence of LPS + IFN α + IL-12 or IL-10 + TGF β (Fig. 9c). LEC-educated cells only became functional effectors when reactivation took place under T_H1-polarizing conditions (LPS + IFN α + IL-12; Fig. 9d), but not in a suppressive setting (IL-10 + TGF β), as demonstrated by their low production of IFN γ and GzB. Importantly, re-stimulation with iDCs in the

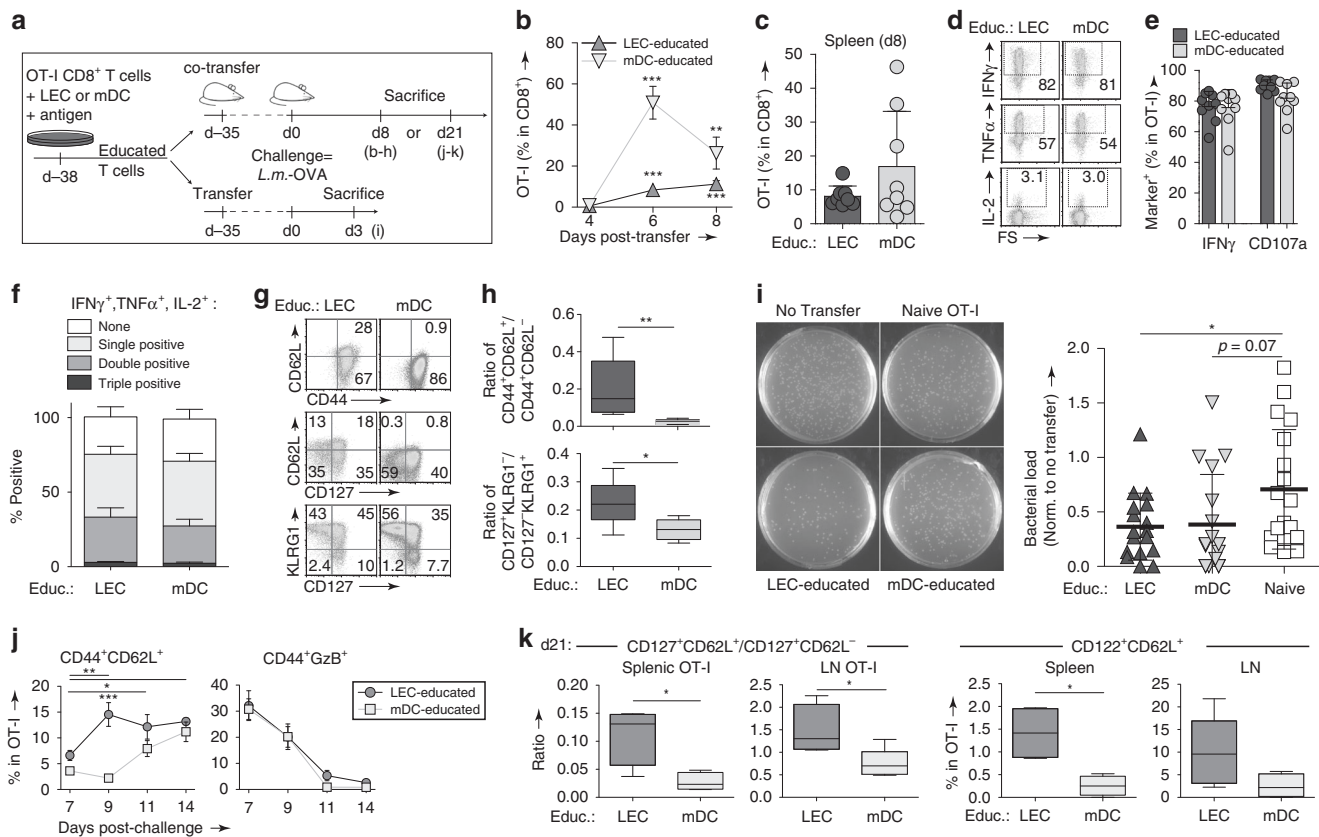


Fig. 8 LEC-educated CD8⁺ T cells protect against infection and give rise to a persistent secondary memory population. **a** Experimental setup: LEC-educated (CD45.1/2⁺) and mDC-educated CD45.1⁺ OT-I cells were co-transferred (1:1, 10⁵ total cells/mouse) into healthy wild-type mice **a–h**, **j**, **k**, and challenged 5 weeks later with *L.m.*-OVA (10³ cfu/mouse i.v.) and sacrificed 8 days **a–h** or 3 weeks later **j**, **k**. **b**, **c** Frequency of OT-I cells among all CD8⁺ T cells in the **b** blood and **c** spleen. **d–h** Splenic OT-I cells were further characterized for: **d** Intracellular staining for IFN γ , TNF α , and IL-2 after ex vivo restimulation; **e** frequency of IFN γ ⁺ and CD107a⁺ cells; **f** frequency of multifunctional (IFN γ , TNF α , and IL-2) cells; **g** expression of CD44, CD62L, CD127, and KLRG1; and **h** (top) ratio of T_{CM} (CD44⁺CD62L⁺) to T_{eff/EM} (CD44⁺CD62L⁻) cells and (bottom) ratio of memory precursor effector cells (CD44⁺CD127⁻KLRG1⁺) to short-lived effector cells (CD44⁺CD127⁻KLRG1⁻). **i** Colony-forming assay performed 3 days following challenge with *L.m.*-OVA (10⁴ cfu/mouse), which occurred 5–9 weeks after adoptive transfer of LEC-educated or mDC-educated OT-I cells, or resting OT-I cells (educ: naïve) as a control. (left) Representative photographs of spleen suspensions from mice receiving indicated OT-I cell populations, cultured on BHI agar plates overnight. (Right) Quantification of bacterial burden, normalized to the c.f.u. detected in the negative control (no transfer) group ($n = 5–6$ per experimental session: 1.5×10^8 c.f.u., 5.6×10^4 c.f.u., and 3.9×10^5 c.f.u. for the three experiments). **j** Kinetics in the frequency of CD44⁺CD62L⁺ and CD44⁺GzB⁺ phenotype on circulating OT-I at the indicated timepoints post-challenge. **k** Ratio of T_{CM} (CD44⁺CD127⁺CD62L⁺) to T_{EM} (CD44⁺CD127⁺CD62L⁻) cells, and percentage of CD122⁺CD62L⁺ cells quantified on OT-I cells at 3 weeks post-challenge. Data points and error bars indicate mean \pm SEM for $n = 8–17$ biological replicates pooled from up to three independent experiments; Boxes indicate median and interquartile range; Whiskers: Min to Max **h**, **k**. * $p \leq 0.05$, ** $p \leq 0.01$, *** $p \leq 0.001$ via one-way ANOVA **b** or by two-way ANOVA **e**, **f**, **j** with Bonferroni’s post-test, or by two-tailed unpaired Student’s *t*-test **c**, **h**, **i**, **k**.

absence of the cognate peptide failed to induce significant levels of IFN γ /GzB in LEC-educated cells under any of the conditions described above, while LPS + IFN α + IL-12 stimulation in the absence of cognate peptide was enough to induce both IFN γ and GzB in mDC-educated cells. Our observations suggest that LEC-educated CD8⁺ T_{CM} cells display antigen specificity and more stringent reactivation requirements compared to conventional DC-educated T_{CM} cells.

Discussion

This study illuminates a new role for LECs in immunomodulation: the generation of antigen-experienced CD8⁺ T cells, which emerge from antigen encounter as memory-like cells. The ability of non-hematopoietic APCs to drive memory formation has been previously reported⁵⁴. In one example, LSEC-educated T cells exhibit an antigen-experienced phenotype with T_{CM}-like characteristics¹⁵. Here, we explored whether by analogy it is feasible that LEC education of naïve CD8⁺ T cells can generate CD8⁺ T cells with multiple differentiation states, including those with

memory-like functional phenotypes. Because LECs are known to be capable of scavenging and cross-presenting exogenous antigen¹⁰, we hypothesized that they may contribute to the generation of memory T cells.

Education of CD8⁺ T cells by LECs versus by professional APCs leads to their acquisition of vastly different phenotypes, which may be dependent on a variety of signals, including TCR affinity, duration of antigen exposure, cytokines, and the balance between co-stimulatory/inhibitory signals, which are all known to regulate the outcomes of T cell differentiation^{55,56}. The conditions of LEC education are characterized by low co-stimulation coupled with inhibitory PD-L1/PD-1 signaling^{7,10}, which are typically observed in transient inflammation and would favor memory rather than terminal effector differentiation. The cytokine milieu in LEC–OT-I co-cultures was consistent with these findings (Supplementary Fig. 2c): we failed to detect IL-12, a key regulator of effector T cell generation that antagonizes memory generation⁵⁷. Notably, we detected IL-7 and IL-15 expressions in LECs (Supplementary Fig. 2d,e), two cytokines known to promote

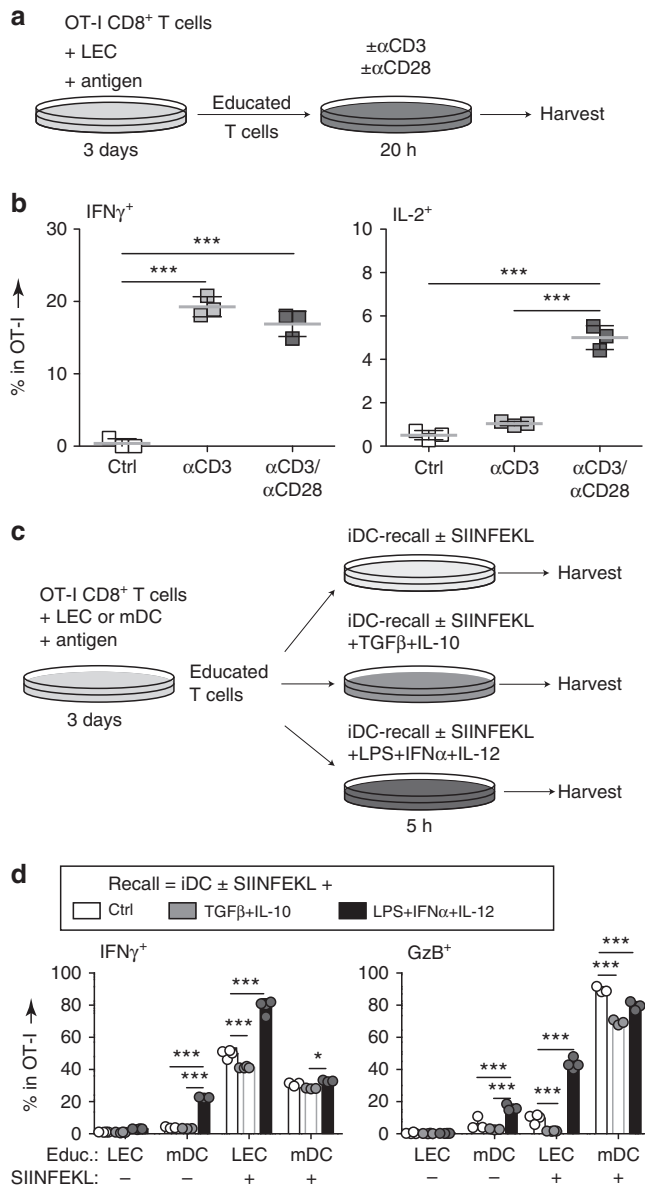


Fig. 9 Stringent requirements for reactivation of LEC-educated CD8⁺ T cells into functional effector cells. **a** Experimental schedule for **b**. LEC-educated OT-I CD8⁺ T cells were re-stimulated with plate-bound CD3 ± CD28 agonist antibodies, and **b** intracellular IFN γ and IL-2 expressions were quantified by flow cytometry as a frequency of live OT-I cells. **c** Experimental schedule for **d**. LEC or mDC-educated OT-I CD8⁺ T cells were re-stimulated with immature DCs (iDCs; pre-pulsed with or without SIINFEKL before co-culture) in the presence of immunogenic (LPS, IFN α , and IL-12) or immunoregulatory (IL-10 and TGF β) cytokines, or iDCs alone (Ctrl) for 5 h. **d** Frequency of IFN γ ⁺ and GzB⁺ (intracellular) cells among live OT-I cells quantified by flow cytometry. Data points and error bars depict mean ± SD for *n* = 3 replicates from one representative of two independent experiments. **p* < 0.05, ***p* < 0.01, ****p* < 0.001 via one-way **b** or two-way **d** ANOVA with Bonferroni's post-test.

the survival, preferential generation, and homeostatic proliferation of functional T_{CM}⁵⁸ and T_{SCM}³⁶ cells.

We further corroborated that LEC-educated CD8⁺ T cells exhibit key functional characteristics of T_{CM} cells³¹. Upon secondary challenge, LEC-educated cells were capable of producing multiple effector cytokines (Fig. 7c, j), and showcased high proliferative and survival capacity even in response to delayed

challenge (Fig. 7i, m). Most importantly, under the correct conditions, LEC-educated T_{CM} cells gave rise to potent cytotoxic lymphocytes that protected the host from pathogen challenge (Fig. 8b–i). Interestingly, LEC-educated cells also appeared to sustain a persistent secondary T_{CM}-like population (Fig. 8g, j, k, Supplementary Fig. 7e, f), showcasing their potential for self-renewal (Supplementary Fig. 8). While we did not confirm if LEC-educated cells exhibit multipotency and self-renewal at the level of individual cells⁵⁹ in similar fashion to canonical T_{SCM}³³ and T_{CM}⁶⁰ cells, LEC-educated cells appeared to be more differentiated than T_{SCM} cells based on CD44 expression, while simultaneously being distinct from effector-like mDC-educated cells (Fig. 4a). Therefore, LEC-educated cells may possess an intermediate differentiation state between T_{SCM} and T_{CM} cells, distinct from terminal effector cells^{61–63}.

We speculate that the functional significance of LEC-educated memory CD8⁺ T cells is their contribution to diversity of memory T cell states. As much as they have in common to conventional T_{CM} cells, they differ in important functional properties. Canonical T_{CM} cells are known to produce IFN γ as a bystander effect during inflammation despite the absence of cognate antigen^{38,64}. In contrast, like naïve cells, LEC-educated cells required all three signals—cognate antigen, co-stimulation, and T_H1-polarizing cytokines, to become reactivated (Fig. 9)⁶⁵. A similar phenomenon was observed for LSEC cross-primed CD8⁺ T cells¹⁵ and in other non-hematopoietic APCs¹⁴, where functional reactivation of antigen-experienced CD8⁺ T cells required multiple synergistic signals. Such prerequisites may safeguard against undesired reactions and hinder the onset of autoimmunity, given that LECs would normally collect endogenous antigens under homeostatic conditions. These key differences may also highlight the need for CD4⁺ T cell help, in the form of co-stimulation or accessory cytokines, to generate canonical T_{CM} cells, although LECs express low levels of co-stimulatory molecules, such as CD80 and CD86 and thereby are unlikely to stimulate optimal CD4⁺ T cell responses^{3,6}.

These more stringent reactivation requirements may be mistaken for tolerance induction by LECs, as reported in tumors and tumor-dLNs⁹. Based on our findings, efficient reactivation of LEC-educated cells and subsequent cytotoxic lymphocyte generation would be quite unlikely in such suppressive microenvironments due to the strong immunoregulatory factors present. After all, the tumor-draining microenvironment rather resembles reactivation in the presence of IL-10 + TGF β , which completely failed to induce functional GzB-expressing effector T cells among LEC-educated cells (Fig. 9d). However, in the setting of chronic inflammation rich in inflammatory cytokines and danger signals, re-stimulation of LEC-educated cells would likely favor generation of cytotoxic effector T cells. Indeed, while controversial, lymphangiogenesis has been frequently associated with aggravation of inflammatory diseases and transplant rejection^{66,67}.

We envision that LEC-educated T_{CM}-like CD8⁺ cells are physiologically significant in at least two scenarios. First, they may be very important in first-line containment against systemic antigen spread. Both viral and bacterial pathogens employ different strategies to circumvent innate immunity, which results in serious pathology⁶⁸. Therefore, LEC priming may spare pathogen-specific T cells from elimination due to first non-immunogenic encounter, generating antigen-experienced cells that may be activated into functional effectors under the correct conditions. A similar role was recently suggested for LSEC-primed CD8⁺ T cells¹⁵. Second, LEC priming may initiate the generation of antigen-experienced CD8⁺ T_{CM}-like cells following infection, because freely draining antigens arrive in the LN much earlier than antigen-loaded migratory DCs from peripheral tissues¹. Consistent with this, in the first moments of a viral

infection, virions were reported to drain to the LN and infect resident cells^{54,69} at the same sub-anatomic locations where LECs are reportedly capable of antigen archiving⁷⁰. Given their constant contact with the antigen-rich pool of the lymph⁷¹, LECs can generate a population of antigen-experienced T cells, which may be readily expanded by activated professional APCs. In line with our hypothesis, stromal cells were able to induce naïve T cell recruitment and activation early during infection, even though their sustained expansion at later time points was markedly limited⁷². Of course, different pathogens engage different immunostimulatory pathways and produce different response kinetics, which directly affect the balance of antigen presentation by professional APCs versus by LECs, possibly explaining seemingly contradictory data with regard to LEC-induced T cell proliferation⁷⁰.

In conclusion, our findings demonstrate a new immunomodulatory role for LECs. Exogenous antigen cross-presentation by LECs induces an expandable pool of memory-like T cells, leading to effector T cell generation under inflammatory conditions to fight an ongoing infection, while preserving a subset of long-lived cells to combat future pathogen encounter. Our work reveals the multifaceted effects of antigen education by LECs, highlighting their dynamic roles in response to the local microenvironment for the regulation of immunity. These findings also help explain and reconcile the seemingly contradictory effects of lymphangiogenesis in tumors versus chronic inflammatory diseases or transplants^{66,67}. As we begin to better understand the impact of antigen presentation by LECs in immunomodulation and unravel the various signals implicated, a new challenge emerges: how can we harness this function to improve protection against pathogens and tumors, or to prevent autoimmunity and transplant rejection?

Methods

Reagents. Chemicals were purchased from Sigma-Aldrich (Buchs, CH) unless otherwise noted. The mature MHC I epitope, OVA₂₅₆₋₂₆₄ (SIINFEKL) peptide, was from GenScript (Piscataway, NJ, USA) and the gp100₂₅₋₃₃ peptide was from Anaspec (Fremont, CA, USA). The Endotoxin-free OVA was from Hyglos GmbH, (Bernried am Starnberger See, DE). Ultra-pure lipopolysaccharide (LPS, 01:11 B4) was from InvivoGen (InvivoGen, San Diego, CA, USA). CpG-B 1826 oligonucleotide (CpG) was obtained from Microsynth (Balgach, CH). Recombinant murine GM-CSF and IL-15 were purchased from Peprotech (Oak Park, CA, USA), IL-10 from eBioscience (Vienna, Austria), IL-12, IFN α and recombinant human TGF β 1 from R&D systems (Minneapolis, MN, USA). Antibodies used in flow cytometry were from BD (Franklin Lakes, NJ, USA), eBioscience (Waltham, MA, USA), or BioLegend (San Diego, CA, USA) unless otherwise noted.

Mice. The following mice strains were used in this study at age 6–12 weeks unless noted otherwise. C57BL/6 (CD45.2 or CD45.1 Ly5) wild-type mice and OT-I CD45.2 transgenic mice, C57BL/6-Tg(TcrAcrb)1100Mjb/J, were purchased from Harlan Laboratories (Gannat, FR). Transgenic OT-I CD45.1/2 mice and OT-3 mice were obtained from Dietmar Zehn. Pmel transgenic mice (B6.Cg-Thy1a/Cy Tg(TcrAcrb)8Rest/J), were a gift from Pedro Romero (Ludwig Institute for Cancer Research, Université de Lausanne). $\beta_2m^{-/-}$ mice (lacking MHC class I) were a gift from Hugh Robson MacDonald. Constitutively OVA-expressing mice (C57BL/6-Tg(CAG-OVA)916Jen/J) were a gift from Anita Chong. Animals were housed in pathogen-free facilities. All procedures and studies involving mice were approved by the Cantonal Veterinary Committee of Vaud, Switzerland (VD2518, VD2981, and VD2992) or the University of Chicago IACUC (protocol # 72414, 72578).

Primary cell isolation. To obtain primary LN LECs and LN FRCs, LNs (axillary, cervical, brachial, inguinal, and popliteal) were digested with 1.3 Wünsch Units/mL Liberase DH and 200 Kunitz/mL DNase I (Roche, Basel, CH) to obtain a single cell suspension and cultured as described⁷³. Cells were cultured for 5 days until confluent, detached by Accutase (Biological Industries, Lucerna-Chem AG, Lucerne CH), and stained with DAPI or PI to exclude dead cells, as well as mAbs against gp38 (clone 8.1.1), CD31 (clone 390), and CD45 (clone 30-F10) and FACS sorted (FACS Aria II, BD, Franklin Lakes, NJ, USA) into the following subpopulations: FRCs (CD45⁻gp38⁺CD31⁻) LECs (CD45⁻gp38⁺CD31⁺), BECs (CD45⁻gp38⁻CD31⁺), and DN (CD45⁻gp38⁻CD31⁻) as described (Supplementary Fig. 9b)⁷⁴. BMDCs were harvested from C57BL/6 mice, differentiated in GM-CSF as described⁷⁵, and used at day 7 of culture. When indicated, BMDCs were matured

(mDCs) by culturing in the presence of antigen (see section below on generation of ex vivo educated CD8⁺ T cells) plus LPS (10 ng/mL) or CpG-B (0.1 μ M) for another 12 h.

For some experiments (Fig. 2), dLNs of i.d. vaccination sites (axillary, brachial, inguinal, and popliteal) were digested in digestion medium (DMEM containing 2% FBS and 2 mM CaCl₂) supplemented with 1 mg/mL collagenase IV and 40 μ g/mL DNase I for 30 min, followed by subsequent digestion in digestion medium supplemented with 3.5 mg/mL collagenase D and 40 μ g/mL for another 30 min as described elsewhere⁷⁶. The resulting cell suspensions were filtered through 70 μ m cell strainers, treated with CD16/CD32 antibody (clone 93) to block nonspecific antibody binding to Fc γ Rs, and then subsequently stained using DAPI, CD45, gp38, and CD31 as indicated above, as well as F4/80 (clone CI:A3-1) and CD11c (clone N418). In addition to LECs and FRCs as indicated earlier, DCs (CD45⁺CD11c⁺F4/80⁻) and macrophages (M ϕ ; CD45⁺CD11c⁻F4/80⁺) were also collected.

Preparation and implantation of LEC spheroids. Primary murine LECs were expanded from WT C57BL/6 or constitutively OVA-expressing mice, and purified via FACS as described above. After sorting, LECs were rested and further expanded on collagen-precoated tissue culture-treated polystyrene Petri dishes, in growth medium (α MEM supplemented with 10% FBS, 100 U/mL penicillin, and 100 μ g/mL streptomycin). LECs were then processed to form spheroids in hanging drop culture as described by Korff⁷⁷. In brief, LECs were detached from plates using Accutase, and then resuspended at 1.0×10^5 cells/mL in growth medium. Sterile methylcellulose (3 mg/mL in α MEM) was mixed into the cell suspension to a final concentration of 0.6 mg/mL. Hanging drops of 20 μ L/droplets were seeded onto the lids of Petri dishes containing PBS, and cultured for at least 3 days until spheroids were visible. Spheroids were collected in 50 mL conical tubes with serum-free IMDM and centrifuged at $20 \times g$ for 5 min at 4 °C, and washed twice to remove excess serum and antibiotics.

Recipient mice were anesthetized under isoflurane (4% induction, 1.5% maintenance) and then laid on their sides. A single 5 mm incision was made on the ventral side of the ear, nearly parallel to the base of the ear, cutting through the cartilage area but without damaging the dorsal dermis. Using a spatula (~4 mm wide by ~20 mm long), an implantation pocket was gently created between the cartilage and the dorsal dermis. Bovine thrombin (~0.01 U in < 5 μ L) was applied to the implantation pocket. At this point, spheroids were mixed with bovine fibrinogen (final concentration of 10 mg/mL in IMDM) and delivered intradermally (i.d.) by pipet into the pocket. After allowing 5 min for gelation, the incision was sealed by applying Histoacryl surgical glue (B. Braun, Melsungen, Germany).

Synthesis of peptide-conjugated nanoparticles (NPs). To explore the mechanisms of cross-presentation poly(propylene sulfide)-NPs with ~30 nm diameter were synthesized and characterized as described²⁹. The long peptide containing the mature MHC I epitope SIINFEKL-Cys-OVA₂₅₀₋₂₆₄ (COVA₂₅₀₋₂₆₄) was synthesized in-house and activated with a 2-pyridylthiol as previously described²⁹. Core sulfhydryl groups on NPs were reacted with the activated peptide and purified on a Sepharose CL6B column (Sigma-Aldrich). Endotoxin levels of antigens were routinely assessed by a colorimetric assay based on the HEK-Blue™ TLR4 cell line (InvivoGen, San Diego, CA, USA) according to the manufacturer's protocol using a standard curve generated from the E-Toxate™ endotoxin standard (Sigma).

Generation of ex vivo LN LEC/mDC-educated CD8⁺ T cells. CD8⁺ T cells from healthy, adult OT-I, OT-3, mice, or Pmel mice were negatively selected from total splenocytes using the EasySep Mouse CD8⁺ T Cell Isolation Kit from Stemcell Technologies (Vancouver, BC, Canada). In some experiments, the resulting CD8⁺ T cells were further purified by FACS based on naïve (CD44⁻CD62L⁺) or VM (CD44⁺) phenotypes. Subsequently, CD8⁺ T-cells were directly co-cultured with LN LECs or mDCs in the presence of either 1 nM NPssCOVA₂₅₀₋₂₆₄, 1 μ M full-length OVA protein, 1 nM SIINFEKL peptide, or 1 μ M of gp100 peptide as indicated (human gp100₂₅₋₃₃; KVPRNQDWL, which differs from the murine sequence by only two amino acids and is functional in reports using murine cells⁷⁸). In some experiments, LN LECs or mDCs were pulsed with antigen, then washed with PBS prior to the addition of T cells. More specifically, 10^4 LECs or DCs were co-cultured with naïve CD8⁺ T cells in 96-well plates for 72 h for OT-I and for 6 days for Pmel CD8⁺ T cells at a ratio of 1:10 APC:T cells in 200 μ L of co-culture media (IMDM with 10% FBS 100 U/mL penicillin, and 100 μ g/mL streptomycin—all from Life Technologies, Carlsbad, CA, USA). Supernatants were harvested and frozen for cytokine analysis. Cells were then processed and stained for immunological markers to be analyzed by flow cytometry (Supplementary Fig. 9c). Cellular proliferation was monitored by CFSE dilution and apoptosis was determined by Annexin V staining (BioVision, Milpitas, CA, USA). T cell proliferation was determined by assessing CFSE intensity using the proliferation algorithm in FlowJo 9.4.11.

In vitro reactivation. LEC/mDC-educated OT-I CD8⁺ T cells were harvested on day 3 of co-culture, washed at least twice with basal medium and counted. 10^5 LEC-educated or mDC-educated CD8⁺ T cells were subsequently co-cultured with fresh 10^4 mDCs loaded with or without the SIINFEKL peptide (1 nM) for 24 h in 200 μ L of co-culture media (mDC-recall). Supernatants were harvested and frozen

for cytokine analysis. Cells were then processed and stained for immunological markers to be analyzed by flow cytometry. The levels of intracellular cytokines were determined after 3 h reactivation and 2 h of Brefeldin A (BfA) treatment. When indicated, LEC-educated or mDC-educated CD8⁺ T cells were reactivated by non-LPS-treated DCs (immature DCs, iDCs) loaded with or without the SIINFEKL peptide (1 nM) for 24 h in the presence or absence of the following cytokines: rmlL-12 (5 ng/mL), rmlFN α (2 kU/mL), rmlIL-10 (60 U/mL), rHTGF β 1 (500 U/mL). In some experiments, reactivation of LEC-educated or mDC-educated CD8⁺ T cells was also conducted with plate-bound anti-CD3 antibody (145.2C11) at 5 μ g/mL and/or soluble anti-CD28 (37.51) at 2 μ g/mL (aCD3/CD28, eBioscience). The same procedures, described above, were performed to analyze the phenotype and function of the reactivated cells.

Antigenic challenge. To determine whether exogenous antigen uptake by LNSCs can drive CD8⁺ T cell proliferation in vivo, we i.d. administered 50 μ g of endotoxin-free OVA in all four limbs at a volume of 10 μ L/limb, or saline as a control. For one study (Fig. 2), a total dose of 100 μ g of endotoxin-free OVA was administered i.d. in six locations, including all four footpads (10 μ L per limb) and two locations along the spinal axis of the mouse in the dorsal skin (30 μ L per spot). To test the capacity of LN LEC/mDC-educated T cells to respond to secondary antigen encounter in vivo, we subcutaneously administered 50 μ g of endotoxin-free OVA plus 100 μ g of ultra-pure LPS.

Infection with OVA-expressing *L.m.* To assess the functional potential of LN LEC/mDC-educated CD8⁺ T cell upon pathogenic challenge, mice were infected i.v. with *L.m.*-OVA⁷⁹ (10³ colony forming units, cfu) acquired from log phase of growth in brain heart infusion (BHI) (Sigma-Aldrich) medium. The mice were challenged at least 5 weeks following adoptive transfer of LN LEC/mDC-educated CD8⁺ T cells. The mice were sacrificed either 8 days after challenge to analyze T cell responses or, 3 weeks after challenge to assess the formation of secondary memory. For the analysis of bacterial load in the spleen, mice were infected with 10⁴ cfu *L.m.*-OVA at least 9 weeks following adoptive transfer of LN LEC/mDC-educated CD8⁺ T cells and sacrificed 3 days after. Spleens were collected, homogenized, and resuspended in 10 mL sterile PBS. Cell suspensions were then plated on BHI agar plates and incubated overnight at 37 °C. The following day, colony-forming units were counted and the amounts of *L.m.*-OVA were calculated with respect to the relative dilutions.

Ex vivo killing assay. To assess the specific killing capacity of reactivated LEC-educated and mDC-educated CD8⁺ T cells, the cells were cultured, following in vivo antigen re-encounter, with a 1:1 mixture of CFSE^{high}-labeled (5 μ M) SIINFEKL-loaded and CFSE^{low}-labeled (0.1 μ M) mismatched-peptide-loaded DCs (mixed target cells) at different effector over target cell ratios. We kept the number of mixed target cells constant at 5 \times 10⁴ cells. Mixed target cells alone served as a control for non-specific death. After 12–16 h, the ratio of the surviving CFSE^{high} and CFSE^{low} cell populations was assessed by flow cytometry to calculate the percentage of specific killing as follows: % specific killing: 100 – [100 \times (CFSE^{high}/CFSE^{low})_{sample} / (CFSE^{high}/CFSE^{low})_{control}].

Flow cytometry. Cells were washed and stained with a cocktail of surface antibodies in staining buffer, containing HBSS (Life Technologies) supplemented with 0.5% bovine serum albumin. Cell viability was determined by propidium iodide incorporation in staining buffer after surface antibody staining or with live/dead fixable cell viability reagent (Life Technologies) in PBS before surface antibody staining. For blocking non-specific binding of immunoglobulin to Fc receptors, cells were also pre-incubated with purified anti-CD16/CD32 antibody (clone 93) for 10 min on ice prior to immunostaining. For intracellular/intranuclear staining, cells were fixed and permeabilized with the Foxp3/Transcription Factor Fixation/Permeabilization kit (eBioscience) according to the manufacturer's instructions. Cells were stained in permeabilization buffer with a cocktail of monoclonal antibodies. For phospho-specific staining, cells were fixed with IC fixation buffer (eBioscience) and subsequently incubated with ice-cold 100% methanol for membrane permeabilization. Cells were stained with a cocktail of surface and phospho-flow antibodies in staining buffer. The following anti-mouse antibodies were used: CD62L (MEL-14), CD44 (IM7), KLRG1 (2F1/KLRG1), PD-1 (RMP1-30), CXCR3 (CXCR3-173), CD43 (1B11), CD27 (LG.3A10), CD122 (TM-b1), CCR7 (4B12), CD127 (A7R34), T-bet (eBio4B10), Eomes (Dan11mag), LFA-1 (H155-78), Sca-1 (D7), Bcl-2 (BCL10C4), CD45.1 (F20), CD45.2 (104), CD8 (53-6.7), CD3e (145-2C11), IFN γ (XMG1.2), IL-2 (JES6-5H4), TNF α (MP6-XT22), CD107 (1D4B), Granzyme-B (NGZB), ki-67 (SolA15), pS6^{S235/236} (D57.2.2E), pmTOR^{S2448} (O21-404), pAkt^{S473} (D9E). Phospho-flow antibodies were from Cell Signaling Technology (Danvers, MA, USA). Finally, cells were resuspended in staining buffer and analyzed by flow cytometry (CyAn ADP Flow Cytometer, DAKO or BD LSRFortessa 5-laser SORP). Data analysis was performed using FlowJo (v9.4, Tree Star Inc., Ashland, OR, USA). Identification of OT-I cells from flow cytometry plots generally followed the gating strategies in Supplementary Fig. 9a, c.

Quantitative real-time RT-PCR. Total RNA was isolated with the RNeasy mini plus Kit (QIAGEN, Hombrechtikon, CH) and reverse transcription was carried out with the iScript cDNA Synthesis Kit (Bio-Rad Laboratories AG, Cressier, CH) according to the manufacturer's instructions. Quantitative RT-PCR was performed using SYBR Green mix and a LightCycler[®] 96 instrument (both Roche). Primer sequences were as follows: IL-7, 5'-TCTCCACTGATCCTTGTTC-3' and 5'-CTTCAACTTGGCAGCAGCAC-3'; IL-15, 5'-GTGACTTTCATCCCAGTTGC-3' and 5'-TTCCTTGACCCAGATTCTG-3'. For isolation from cells in culture, cells were pelleted and directly used. For RNA isolation from control and inflamed skin-dLNs of C57Bl/6 mice, draining LN were isolated from mice 5 days after i.d. injection with either PBS or 15 μ g of CpG-B in all four limbs at a volume of 10 μ L/limb.

RNA sequencing. RNA sequencing was conducted with naïve or LEC/mDC-educated CD8⁺ T cells, coming from 3 OT-I mice, at three different time points during co-culture (day 1, 2, 3), making for a total of 21 samples across seven different conditions. Total RNA was extracted with the RNeasy mini Plus Kit (Qiagen, Hombrechtikon, CH). The Agilent RNA ScreenTape assay was performed in combination with the 4200 TapeStation system (Agilent Technologies) for the determination of quality and quantity of the RNA samples. Additionally, concentration of the RNA samples was determined with Qubit and NanoDrop (both ThermoFisher Scientific, Waltham, MA, USA). Sequencing libraries were generated with a TruSeq Stranded mRNA Prep Kit (Illumina, San Diego, USA) according to manufacturer's protocols. The libraries were quantified by Qubit DNA HS and profile analysis was performed by Fragment Analyzer (Advanced Analytical). Seven samples were then pooled for each sequencing run (Illumina NextSeq 500) with 400 million reads (nominally ~55 million reads/sample) of 75 bps in single-end mode.

Transcriptional profile analysis. Raw-sequencing files were first checked for sequence quality and potential contamination using the FastQC program (Babraham Bioinformatics, Cambridge, United Kingdom). From here, read mapping and read counting was performed on the HTSStation platform⁸⁰, which is an integrated modular platform using the Bowtie2 algorithm to map reads to a reference mouse genome⁸¹ and the (Bioconductor) Limma.R package⁸² to perform differential expression statistical analyses⁸³ and generation of adjusted *p*-values values via one-way ANOVA, adjusting for the false-discovery rate using the Benjamini–Hochberg method.

To visualize global changes in gene expression as a function of T cell education and time, we applied PCA on all 45,707 detected genes, and hierarchical clustering on a pre-filtered subset of these genes with a median rpkm >5, and with adjusted *p* < 0.01 versus expression on naïve OT-I cells. This subset of 16,752 genes essentially represented substantially expressed genes that were differentially regulated in naïve or in antigen-experienced CD8⁺ T cells. The rpkm of these 16,752 genes were submitted to the GENE-E platform (<https://software.broadinstitute.org/GENE-E/index.html>) for hierarchical clustering, using Pearson correlation coefficients among the genes to potentially identify modules of genes that appear co-regulated or induced uniquely due to LEC- or mDC education.

To compare data expression in LEC-educated cells with memory/effector cell gene signatures, the genes with the greatest differences in expression (all of those with an adjusted *p* value of <0.05) and a change in expression of >1.5-fold between day 3 LEC/mDC-educated cells) were selected. To detect genes most differentially regulated in LEC-educated cells on day 3, we selected genes that fulfilled the following conditions: (1) an adjusted *p* < 0.01 between any pair of comparisons among naïve OT-I cells and LEC-educated or mDC-educated OT-I on day 3, and (2) |log₂FC| ≥ 2.89-fold difference in expression between LEC-educated versus mDC-educated OT-I cells. These criteria led to a final panel of ~200 genes, which represent the genes that are differentially regulated in antigen-experienced T cells, and furthermore, most differentially modulated by the nature of the APC used (Supplementary Table 1). These ~200 genes were mapped onto biological functions and pathways using Gene Ontology Enrichment Analysis (Gene Ontology Consortium—<http://geneontology.org/>). Furthermore, we used the Gene Ontology Atlas⁴⁷ to build lists of genes related to specific biological processes, and used R and Excel to map these genes on the volcano plots to better visualize gene expression patterns between naïve OT-I cells, or LEC-educated or mDC-educated OT-I cells.

Statistical analysis. Statistical analysis was performed using one-way or two-way analysis of variance (ANOVA) or unpaired, two-tailed Student's *t*-test followed by Bonferroni post-test with Prism 5 software (Graphpad, San Diego, CA, USA) unless otherwise stated. If the groups to be compared had significantly different variances (*p* < 0.05 by *F* test) then Welch's correction was performed. In all the animal studies, mice were randomly assigned to the different groups and treated in a random order. The investigators were not blinded to group allocation during the experiment or when assessing the outcome. The number of animals chosen per experiment was based on previous publications using similar models and addressing similar questions, as well as on previous studies performed in our lab when statistical significance was actually achieved. To account for data reproducibility, the experiments were performed at least twice. For in vitro experiments, samples were randomly assigned to positions in multi-well plates and the processing order was random. The investigators were not blinded to sample identity. Sample sizes were chosen as the minimum number of

mice to sort enough cells to perform three to four technical replicates per group per assay. Results are shown as mean \pm standard deviation, unless noted otherwise, with significance indicated as $*p \leq 0.05$, $**p \leq 0.01$, and $***p \leq 0.001$. When Box-and-Whiskers plots are used, the line in the middle of the box indicates the median and the whiskers go down to the smallest and up to the largest value.

Reporting summary. Further information on research design is available in the Nature Research Reporting Summary linked to this article.

Data availability

The RNA sequencing data have been deposited to the NIH Gene Expression Omnibus under accession number GSE88830. Source data are provided as a Source Data file. All other data are included in the supplemental information or available from the authors upon reasonable request.

Received: 12 December 2018; Accepted: 19 December 2019;

Published online: 27 January 2020

References

- Hirosue, S. & Dubrot, J. Modes of antigen presentation by lymph node stromal cells and their immunological implications. *Front. Immunol.* **6**, 446 (2015).
- Malhotra, D., Fletcher, A. L. & Turley, S. J. Stromal and hematopoietic cells in secondary lymphoid organs: partners in immunity. *Immunol. Rev.* **251**, 160–176 (2013).
- Card, C. M., Yu, S. S. & Swartz, M. A. Emerging roles of lymphatic endothelium in regulating adaptive immunity. *J. Clin. Invest.* **124**, 943–952 (2014).
- Turley, S. J., Fletcher, A. L. & Elpek, K. G. The stromal and haematopoietic antigen-presenting cells that reside in secondary lymphoid organs. *Nat. Rev. Immunol.* **10**, 813–825 (2010).
- Podgrabinska, S. & Skobe, M. Role of lymphatic vasculature in regional and distant metastases. *Microvasc. Res.* **95**, 46–52 (2014).
- Dubrot, J. et al. Lymph node stromal cells acquire peptide-MHCII complexes from dendritic cells and induce antigen-specific CD4⁺ T cell tolerance. *J. Exp. Med.* **211**, 1153–1166 (2014).
- Tewalt, E. F. et al. Lymphatic endothelial cells induce tolerance via PD-L1 and lack of costimulation leading to high-level PD-1 expression on CD8 T cells. *Blood* **120**, 4772–4782 (2012).
- Cohen, J. N. et al. Lymph node-resident lymphatic endothelial cells mediate peripheral tolerance via Aire-independent direct antigen presentation. *J. Exp. Med.* **207**, 681–688 (2010).
- Lund, A. W. et al. VEGF-C promotes immune tolerance in B16 melanomas and cross-presentation of tumor antigen by lymph node lymphatics. *Cell Rep.* **1**, 191–199 (2012).
- Hirosue, S. et al. Steady-state antigen scavenging, cross-presentation, and CD8⁺ T cell priming: a new role for lymphatic endothelial cells. *J. Immunol.* **192**, 5002–5011 (2014).
- Mueller, D. L. Mechanisms maintaining peripheral tolerance. *Nat. Immunol.* **11**, 21–27 (2010).
- Redmond, W. L. & Sherman, L. A. Peripheral tolerance of CD8 T lymphocytes. *Immunity* **22**, 275–284 (2005).
- Schietinger, A., Delrow, J. J., Basom, R. S., Blattman, J. N. & Greenberg, P. D. Rescued tolerant CD8 T cells are preprogrammed to reestablish the tolerant state. *Science* **335**, 723–727 (2012).
- Vezys, V., Olson, S. & Lefrançois, L. Expression of intestine-specific antigen reveals novel pathways of CD8 T cell tolerance induction. *Immunity* **12**, 505–514 (2000).
- Böttcher, J. P. et al. Liver-primed memory T cells generated under noninflammatory conditions provide anti-infectious immunity. *Cell Rep.* **3**, 779–795 (2013).
- Ahlers, J. D. & Belyakov, I. M. Memories that last forever: strategies for optimizing vaccine T-cell memory. *Blood* **115**, 1678–1689 (2010).
- Kurtulus, S., Tripathi, P. & Hildeman, D. A. Protecting and rescuing the effectors: roles of differentiation and survival in the control of memory T cell development. *Front. Immunol.* **3**, 404 (2012).
- Harty, J. T. & Badovinac, V. P. Shaping and reshaping CD8⁺ T-cell memory. *Nat. Rev. Immunol.* **8**, 107–119 (2008).
- Joshi, N. S. & Kaech, S. M. Effector CD8 T cell development: a balancing act between memory cell potential and terminal differentiation. *J. Immunol.* **180**, 1309–1315 (2008).
- Fletcher, A. L. et al. Lymph node fibroblastic reticular cells directly present peripheral tissue antigen under steady-state and inflammatory conditions. *J. Exp. Med.* **207**, 689–697 (2010).
- Merad, M. et al. Langerhans cells renew in the skin throughout life under steady-state conditions. *Nat. Immunol.* **3**, 1135–1141 (2002).
- Stoitzner, P. et al. Langerhans cells cross-present antigen derived from skin. *Proc. Natl. Acad. Sci. USA* **103**, 7783–7788 (2006).
- Flacher, V. et al. Murine Langerin⁺ dermal dendritic cells prime CD8⁺ T cells while Langerhans cells induce cross-tolerance. *EMBO Mol. Med.* **6**, 1191–1204 (2014).
- Roozendaal, R. et al. Conduits mediate transport of low-molecular-weight antigen to lymph node follicles. *Immunity* **30**, 264–276 (2009).
- Gerner, M. Y., Torabi-Parizi, P. & Germain, R. N. Strategically localized dendritic cells promote rapid T cell responses to lymph-borne particulate antigens. *Immunity* **42**, 172–185 (2015).
- Itano, A. A. et al. Distinct dendritic cell populations sequentially present antigen to CD4 T cells and stimulate different aspects of cell-mediated immunity. *Immunity* **19**, 47–57 (2003).
- Onder, L. et al. IL-7-producing stromal cells are critical for lymph node remodeling. *Blood* **120**, 4675–4683 (2012).
- Miller, C. N. et al. IL-7 production in murine lymphatic endothelial cells and induction in the setting of peripheral lymphopenia. *Int. Immunol.* **25**, 471–483 (2013).
- Hirosue, S., Kourtis, I. C., van der Vlies, A. J., Hubbell, J. A. & Swartz, M. A. Antigen delivery to dendritic cells by poly(propylene sulfide) nanoparticles with disulfide conjugated peptides: cross-presentation and T cell activation. *Vaccine* **28**, 7897–7906 (2010).
- Obar, J. J. & Lefrançois, L. Memory CD8⁺ T cell differentiation. *Ann. N. Y. Acad. Sci.* **1183**, 251–266 (2010).
- Wherry, E. J. et al. Lineage relationship and protective immunity of memory CD8 T cell subsets. *Nat. Immunol.* **4**, 225–234 (2003).
- Kaech, S. M. & Cui, W. Transcriptional control of effector and memory CD8⁺ T cell differentiation. *Nat. Rev. Immunol.* **12**, 749–761 (2012).
- Gattinoni, L. et al. A human memory T cell subset with stem cell-like properties. *Nat. Med.* **17**, 1290–1297 (2011).
- Zhang, Y., Joe, G., Hexner, E., Zhu, J. & Emerson, S. G. Host-reactive CD8⁺ memory stem cells in graft-versus-host disease. *Nat. Med.* **11**, 1299–1305 (2005).
- Farber, D. L., Yudanin, N. A. & Restifo, N. P. Human memory T cells: generation, compartmentalization and homeostasis. *Nat. Rev. Immunol.* **14**, 24–35 (2014).
- Cieri, N. et al. IL-7 and IL-15 instruct the generation of human memory stem T cells from naive precursors. *Blood* **121**, 573–584 (2013).
- Enouz, S., Carrié, L., Merkler, D., Bevan, M. J. & Zehn, D. Autoreactive T cells bypass negative selection and respond to self-antigen stimulation during infection. *J. Exp. Med.* **209**, 1769–1779 (2012).
- Haluszczak, C. et al. The antigen-specific CD8⁺ T cell repertoire in unimmunized mice includes memory phenotype cells bearing markers of homeostatic expansion. *J. Exp. Med.* **206**, 435–448 (2009).
- Böttcher, J. & Knolle, P. A. Global transcriptional characterization of CD8⁺ T cell memory. *Semin. Immunol.* **27**, 4–9 (2015).
- Crotty, S., Johnston, R. J. & Schoenberger, S. P. Effectors and memories: Bcl-6 and Blimp-1 in T and B lymphocyte differentiation. *Nat. Immunol.* **11**, 114–120 (2010).
- Wirth, T. C. et al. Repetitive antigen stimulation induces stepwise transcriptome diversification but preserves a core signature of memory CD8⁺ T cell differentiation. *Immunity* **33**, 128–140 (2010).
- Tolkdorf, F. et al. The PDL1-inducible GTPase Arl4d controls T effector function by limiting IL-2 production. *Sci. Rep.* **8**, 16123 (2018).
- Scholz, G. et al. Modulation of mTOR signalling triggers the formation of stem cell-like memory T cells. *EBioMedicine* **4**, 50–61 (2016).
- Choi, U. Y. et al. Tripartite motif-containing protein 30 modulates TCR-activated proliferation and effector functions in CD4⁺ T cells. *PLoS One* **9**, e95805 (2014).
- Bai, A., Hu, H., Yeung, M. & Chen, J. Kruppel-like factor 2 controls T cell trafficking by activating L-selectin (CD62L) and sphingosine-1-phosphate receptor 1 transcription. *J. Immunol.* **178**, 7632–7639 (2007).
- Best, J. A. et al. Transcriptional insights into the CD8⁺ T cell response to infection and memory T cell formation. *Nat. Immunol.* **14**, 404–412 (2013).
- The Gene Ontology Consortium. Gene Ontology Consortium: going forward. *Nucleic Acids Res.* **43**, D1049–D1056 (2015).
- Chang, J. T., Wherry, E. J. & Goldrath, A. W. Molecular regulation of effector and memory T cell differentiation. *Nat. Immunol.* **15**, 1104–1115 (2014).
- Araki, K. et al. mTOR regulates memory CD8 T-cell differentiation. *Nature* **460**, 108–112 (2009).
- Pollizzi, K. N. et al. mTORC1 and mTORC2 selectively regulate CD8⁺ T cell differentiation. *J. Clin. Invest.* **125**, 2090–2108 (2015).
- von Andrian, U. H. & Mempel, T. R. Homing and cellular traffic in lymph nodes. *Nat. Rev. Immunol.* **3**, 867–878 (2003).
- Kastenmuller, W. et al. Peripheral prepositioning and local CXCL9 chemokine-mediated guidance orchestrate rapid memory CD8⁺ T cell responses in the lymph node. *Immunity* **38**, 502–513 (2013).

53. Sung, J. H. et al. Chemokine guidance of central memory T cells is critical for antiviral recall responses in lymph nodes. *Cell* **150**, 1249–1263 (2012).
54. Bassett, J. D. et al. CD8⁺ T-cell expansion and maintenance after recombinant adenovirus immunization rely upon cooperation between hematopoietic and nonhematopoietic antigen-presenting cells. *Blood* **117**, 1146–1155 (2011).
55. Williams, M. A. & Bevan, M. J. Effector and memory CTL differentiation. *Annu. Rev. Immunol.* **25**, 171–192 (2007).
56. Zehn, D., Roepke, S., Weakly, K., Bevan, M. J. & Prlic, M. Inflammation and TCR signal strength determine the breadth of the T cell response in a bim-dependent manner. *J. Immunol.* **192**, 200–205 (2014).
57. Cui, W., Joshi, N. S., Jiang, A. & Kaech, S. M. Effects of Signal 3 during CD8 T cell priming: Bystander production of IL-12 enhances effector T cell expansion but promotes terminal differentiation. *Vaccine* **27**, 2177–2187 (2009).
58. Kaneko, S. et al. IL-7 and IL-15 allow the generation of suicide gene-modified alloreactive self-renewing central memory human T lymphocytes. *Blood* **113**, 1006–1015 (2009).
59. Buchholz, V. R., Gräf, P. & Busch, D. H. The smallest unit: effector and memory CD8⁺ T cell differentiation on the single cell level. *Front. Immunol.* **4**, 31 (2013).
60. Graef, P. et al. Serial transfer of single-cell-derived immunocompetence reveals stemness of CD8⁺ central memory T cells. *Immunity* **41**, 116–126 (2014).
61. Ahmed, R., Bevan, M. J., Reiner, S. L. & Fearon, D. T. The precursors of memory: models and controversies. *Nat. Rev. Immunol.* **9**, 662–668 (2009).
62. Lefrançois, L. & Marzo, A. L. The descent of memory T-cell subsets. *Nat. Rev. Immunol.* **6**, 618–623 (2006).
63. Gattinoni, L., Klebanoff, C. A. & Restifo, N. P. Paths to stemness: building the ultimate antitumour T cell. *Nat. Rev. Cancer* **12**, 671–684 (2012).
64. Kambayashi, T., Assarsson, E., Lukacher, A. E., Ljunggren, H.-G. & Jensen, P. E. Memory CD8⁺ T cells provide an early source of IFN- γ . *J. Immunol.* **170**, 2399–2408 (2003).
65. Boesteanu, A. C. & Katsikis, P. D. Memory T cells need CD28 costimulation to remember. *Semin. Immunol.* **21**, 69–77 (2009).
66. Swartz, M. A. Inflammatory lymphangiogenesis in postpartum breast tissue remodeling. *J. Clin. Invest.* **124**, 3704–3707 (2014).
67. Angeli, V. & Randolph, G. J. Inflammation, lymphatic function, and dendritic cell migration. *Lymphatic Res. Biol.* **4**, 217–228 (2006).
68. Finlay, B. B. & McFadden, G. Anti-immunology: evasion of the host immune system by bacterial and viral pathogens. *Cell* **124**, 767–782 (2006).
69. Hickman, H. D. et al. Direct priming of antiviral CD8⁺ T cells in the peripheral interfollicular region of lymph nodes. *Nat. Immunol.* **9**, 155–165 (2008).
70. Tamburini, B. A., Burchill, M. A. & Kedl, R. M. Antigen capture and archiving by lymphatic endothelial cells following vaccination or viral infection. *Nat. Commun.* **5**, 3989 (2014).
71. Clement, C. C., Rotzschke, O. & Santambrogio, L. The lymph as a pool of self-antigens. *Trends Immunol.* **32**, 6–11 (2011).
72. Thomas, S., Kolumam, G. A. & Murali-Krishna, K. Antigen presentation by nonhemopoietic cells amplifies clonal expansion of effector CD8 T cells in a pathogen-specific manner. *J. Immunol.* **178**, 5802–5811 (2007).
73. Fletcher, A. L. et al. Reproducible isolation of lymph node stromal cells reveals site-dependent differences in fibroblastic reticular cells. *Front. Immunol.* **2**, 1–15 (2011).
74. Link, A. et al. Fibroblastic reticular cells in lymph nodes regulate the homeostasis of naive T cells. *Nat. Immunol.* **8**, 1255–1265 (2007).
75. Lutz, M. B. et al. An advanced culture method for generating large quantities of highly pure dendritic cells from mouse bone marrow. *J. Immunol. Methods* **223**, 77–92 (1999).
76. Broggi, M., Schmalzer, M. & Lagarde, N. Isolation of murine lymph node stromal cells. *J. Vis. Exp.* **19**, e51803 (2014).
77. Korff T. Three-Dimensional Spheroid Culture of Endothelial Cells. In *Methods in Endothelial Cell Biology* (ed. Augustin, H. G.) Ch. 6 (Springer, Berlin, 2004).
78. Overwijk, W. W. et al. gp100/pmel 17 is a murine tumor rejection antigen: induction of “self-”reactive, tumoricidal T cells using high-affinity, altered peptide ligand. *J. Exp. Med.* **188**, 277–286 (1998).
79. Pope, C. et al. Organ-specific regulation of the CD8 T cell response to *Listeria monocytogenes* infection. *J. Immunol.* **166**, 3402–3409 (2001).
80. David, F. P. A. et al. HTSstation: a web application and open-access libraries for high-throughput sequencing data analysis. *PLoS One* **9**, e85879 (2014).
81. Langmead, B., Trapnell, C., Pop, M. & Salzberg, S. L. Ultrafast and memory-efficient alignment of short DNA sequences to the human genome. *Genome Biol.* **10**, R25 (2009).
82. Ritchie, M. E. et al. limma powers differential expression analyses for RNA-sequencing and microarray studies. *Nucleic Acids Res.* **43**, e47–e47 (2015).
83. Anders, S. & Huber, W. Differential expression analysis for sequence count data. *Genome Biol.* **11**, R106 (2010).

Acknowledgements

The authors are grateful to Yue Wang, Yassin Ben Saida, Xavier Quaglia-Thermes, Giacomo O. Diaceri, Vasiliki Panagiotou, S. Oberle, Cristina Cartoni, E. Anastasiou, Elena Cabello, the EPFL Flow Cytometry Core Facility (Miguel Garcia, Loïc Tauzin, Valérie Glutz) and the University of Chicago Cytometry and Antibody Technology Core (David Leclerc, Mandel Davis, Mike Olson, and Robert Ladd) for technical support and assistance, as well as Maria-Luisa Alegre, Bana Jabri, Albert Bendelac, Amanda W. Lund, Catherine M. Card and Eleonora Simeoni for helpful discussions and suggestions. This work was funded by grants from the Swiss Cancer Research (KFS-3312-08-2013 to M.A.S.), the European Research Council (AdG-323053 to M.A.S.), and the National Institutes of Health (R01 CA219304-01A1 to M.A.S.).

Author contributions

Conceptualization: E.V., S. Hirosue, S. Hugues, M.A.S. Methodology: E.V., S.S.Y., S. Hirosue, M.R.R., F.d.V.D., S.S., W.W.K., A.M., D.Z., S. Hugues, M.A.S. Investigation: E.V., S.S.Y., S. Hirosue, P.C.H., M.A.S. Validation: S.S.Y., S. Hirosue, A.M., D.Z., S. Hugues, M.A.S. Analysis: E.V., S.S.Y., P.C.-H., M.A.S. Resources: D.Z., S. Hugues, M.A.S. Supervision: M.A.S. First draft: E.V. Revisions: E.V., S.S.Y., M.A.S. Visualization: E.V., S.S.Y. Project administration: M.A.S. Supervision: M.A.S. Funding acquisition: M.A.S.

Competing interests

The authors declare no competing interests.

Additional information


Supplementary information is available for this paper at <https://doi.org/10.1038/s41467-019-14127-9>.

Correspondence and requests for materials should be addressed to M.A.S.

Peer review information *Nature Communications* thanks the anonymous reviewer(s) for their contribution to the peer review of this work.

Reprints and permission information is available at <http://www.nature.com/reprints>

Publisher's note Springer Nature remains neutral with regard to jurisdictional claims in published maps and institutional affiliations.

 **Open Access** This article is licensed under a Creative Commons Attribution 4.0 International License, which permits use, sharing, adaptation, distribution and reproduction in any medium or format, as long as you give appropriate credit to the original author(s) and the source, provide a link to the Creative Commons license, and indicate if changes were made. The images or other third party material in this article are included in the article's Creative Commons license, unless indicated otherwise in a credit line to the material. If material is not included in the article's Creative Commons license and your intended use is not permitted by statutory regulation or exceeds the permitted use, you will need to obtain permission directly from the copyright holder. To view a copy of this license, visit <http://creativecommons.org/licenses/by/4.0/>.

© The Author(s) 2020